

From complexity geometry to holographic spacetime

Johanna Erdmenger^{*} and Anna-Lena Weigel[†]

*Institute for Theoretical Physics and Astrophysics and Würzburg-Dresden Cluster of Excellence ct.qmat,
Julius-Maximilians-Universität Würzburg, 97074 Würzburg, Germany*

Marius Gerbershagen[‡]

*Theoretische Natuurkunde, Vrije Universiteit Brussel (VUB) and The International Solvay Institutes,
Pleinlaan 2, 1050 Brussels, Belgium*

Michal P. Heller[§]

Department of Physics and Astronomy, Ghent University, 9000 Ghent, Belgium



(Received 23 February 2023; accepted 12 September 2023; published 27 November 2023)

An important conjecture within the AdS/CFT correspondence relates holographic spacetime to the quantum computational complexity of the dual quantum field theory. However, the quantitative understanding of this relation is largely an open question. In this work, to address this question we establish a map between a computational complexity measure and its holographic counterpart from first principles. We consider quantum circuits built out of conformal transformations in two-dimensional conformal field theory and a complexity measure based on assigning a cost to quantum gates via the Fubini-Study distance. We find a novel geometric object in three-dimensional anti-de Sitter spacetimes that is dual to this distance. This duality also provides a more general map between holographic geometry of anti-de Sitter universes and complexity geometry as defined in information theory, in which each point represents a state and distances between states are measured by the Fubini-Study metric. We apply the newly found duality to the eternal black hole spacetime and discuss both the origin of linear growth of complexity and the switchback effect within our approach.

DOI: [10.1103/PhysRevD.108.106020](https://doi.org/10.1103/PhysRevD.108.106020)

I. INTRODUCTION

The question of assigning cost to state preparation in holography [1–3] has received significant attention in recent years, building on a conjecture by Susskind relating cost assignment to black hole physics [4]. The focal notion in this context has been computational complexity, a quantity from quantum information counting how many computation steps are necessary to prepare a certain target state from a fixed reference state [5,6]. In chaotic systems of finite size, computational complexity is expected to show a number of features that are universal, in the sense that they hold for any chaotic system and any reasonable definition of complexity. These expected universal features were

conjectured to be related to geometric features of anti-de Sitter (AdS) black hole geometries in [4]. They involve the growth of the size of black hole interiors with time. In line with the universality expectation, these features are probed by many gravity observables. The most prominently studied holographic complexity proposals are the so-called “complexity = volume” [4,7], “complexity = action” [8,9], and “complexity = volume 2.0” [10] proposals. Recently, an infinite class of such gravitational observables was put forward under the slogan “complexity = anything” [11,12]. Moreover, the holographic complexity proposals triggered progress on computational complexity within quantum field theory (QFT) (see [6] for a review). However, up to now the relation to holographic complexity is restricted to qualitative comparisons, due to the fact that soluble examples are either free QFTs or models lacking control over either the boundary or the bulk side.

The main result of our work is a general construction method for gravity duals of the building blocks of computational complexity in QFT, that is quantum circuits and cost functions. We propose for the first time a map between computational complexity in conformal field theories (CFTs) and a geometric object in the gravity theory that

^{*}erdmenger@physik.uni-wuerzburg.de

[†]anna-lena.weigel@physik.uni-wuerzburg.de

[‡]maris.gerbershagen@vub.be

[§]michal.p.heller@ugent.be

Published by the American Physical Society under the terms of the Creative Commons Attribution 4.0 International license. Further distribution of this work must maintain attribution to the author(s) and the published article’s title, journal citation, and DOI. Funded by SCOAP³.

is constructed from first principles, with time evolution built into the gravity dual in a Lorentz covariant way. This map can be naturally applied to the most relevant case—AdS black hole spacetimes and dual thermofield double (TFD) states [13]. Conceptually, our approach extends the known relation between information and geometry for finite Hilbert spaces, as given by Nielsen’s realization [14] of discrete complexity measures by group geodesics, to AdS/CFT.

Much of the previous work on computational complexity in QFTs is based on the framework proposed by Nielsen in [14] to bound complexity of discrete circuits using differential geometry tools. Instead of counting discrete gates that belong to the native quantum computing language, in the Nielsen approach the circuit evolution proceeds in a continuous manner by applying a path ordered exponential,

$$|\psi(\tau)\rangle = \mathcal{P} \exp \left(i \int_0^\tau d\tau' Q(\tau') \right) |\psi(0)\rangle. \quad (1)$$

Different circuits performing the same task are distinguished by a cost function $F[|\psi(\tau)\rangle, Q(\tau)]$ that measures how expensive the application of $Q(\tau)$ onto the state $|\psi(\tau)\rangle$ is. Such a cost function can be viewed as weighting components of $Q(\tau)$ in a basis of generators of infinitesimal gates viewed as ultimate circuit building blocks. The complexity is then defined as the minimum of the total cost,

$$C = \min \int_0^{\tau_f} d\tau F[|\psi(\tau)\rangle, Q(\tau)], \quad (2)$$

subject to the condition that they connect fixed reference $|\psi(0)\rangle$ and target $|\psi(\tau_f)\rangle$ states. A cost function F defines a *Finsler geometry* [14] if it is smooth, positive, positively homogeneous of degree one in its second argument and obeys the triangle inequality. In this case, the target and reference states are represented by manifold points and the complexity by the length of the shortest path between them, i.e. by the geodesic. The following question then arises naturally:

How is this auxiliary complexity geometry for properly understood circuits in holographic QFTs encoded in the gravity dual description?

This important question is addressed in the present work. There are three key conceptual problems that we have to consider in view of answering this question: What is meant by τ in holography? What constitutes a gate set in a QFT? What QFT cost functions can be interpreted holographically? In our proposal we are guided by the observation that the only interface to translate between the boundary and the bulk comes from the identification of source terms in path integrals in holographic QFTs with asymptotic boundary conditions for bulk fields [2,3,15,16]. Therefore, it is natural to identify the circuit parameter τ with the physical time t at the boundary [17],

$$\tau \equiv t. \quad (3)$$

As a consequence, the circuit generator $Q(\tau)$ has to be identified with the physical Hamiltonian $H(t)$,

$$Q(\tau) \equiv H(t). \quad (4)$$

Different QFT source configurations correspond to controllable modifications of the Hamiltonian obtained by adding local primary operators. Therefore, these operators constitute natural generators of the infinitesimal gates. Moreover, constant t slices naturally define states. Considering such slices therefore naturally introduces reference and target states $|\psi(0)\rangle$ and $|\psi(\tau_f)\rangle$. This perspective on obtaining gravity duals for a quantum circuits was outlined in our previous work [17]. Here, we take the crucial further step of connecting the gravity duals of quantum circuits with notions of computational complexity.

We apply this general method to the example of a computational complexity definition based on the Fubini-Study distance as cost function. The Fubini-Study distance is a natural distance measure in Hilbert space. For two infinitesimally separated states $|\psi\rangle$ and $|\psi\rangle + |\delta\psi\rangle$, it takes the form,

$$ds_{\text{FS}}^2 = \frac{\langle \delta\psi | \delta\psi \rangle}{\langle \psi | \psi \rangle} - \frac{\langle \delta\psi | \psi \rangle \langle \psi | \delta\psi \rangle}{\langle \psi | \psi \rangle^2}. \quad (5)$$

The Fubini-Study distance is the unique Riemannian metric on projective Hilbert space¹ invariant under unitary transformations [18]. The geodesic distance θ between two states $|\psi(t_1)\rangle$ and $|\psi(t_2)\rangle$ for this metric is given by (see Fig. 1)

$$\cos(\theta)^2 = \frac{\langle \psi(t_1) | \psi(t_2) \rangle \langle \psi(t_2) | \psi(t_1) \rangle}{\langle \psi(t_1) | \psi(t_1) \rangle \langle \psi(t_2) | \psi(t_2) \rangle}, \quad (6)$$

which implies that θ is bounded from above by $\pi/2$.

How can this ansatz define a nontrivial complexity measure? The answer to this question relies on the fact that due to restricting to Hamiltonians obtained by turning on specific sources, we cannot move along some of the directions in the Hilbert space and therefore the shortest path is not necessarily a geodesic. In other words, by only allowing directions corresponding to a subset of source deformations in the QFT, we assign infinite cost to the other Hilbert space directions. Moreover, we define the cost function to be the square of the Fubini-Study line element,

¹The projective Hilbert space arises from identifying $|\psi\rangle \sim \alpha|\psi\rangle$ for $\alpha \in \mathbb{C}$, i.e. it is the space of properly normalized physically indistinguishable Hilbert space elements.

$$F_{\text{FS}} = ds_{\text{FS}}^2. \quad (7)$$

This is a slight departure from the formalism of [14], as it implies that the cost function is not positively homogeneous of degree one and hence does not define a Finsler metric in our setup. However, similar notions of complexity associated to cost functions which are positively homogeneous of degree greater than one were introduced into the computational complexity setup for QFTs in [19] with the justification that it provides a better match to the “complexity = volume” proposal² (see also [22–24] for further discussion on the merits and drawbacks of this choice). For us, choosing the cost function as the square of the Fubini-Study line element simplifies the dual bulk description while also allowing for a complexity measure that fulfills important properties postulated to hold for complexity measures in the AdS/CFT setting, as we will see in the following.

A key insight of our present work comes from recognizing that the holographic dictionary naturally provides information about overlaps of states and, related to them, correlation functions. The Fubini-Study cost function utilizes precisely this information, as it reduces to the variance of $H(t)$ when applied to one layer of the circuit (1),

$$F_{\text{FS}} = \langle \psi(t) | H(t)^2 | \psi(t) \rangle - \langle \psi(t) | H(t) | \psi(t) \rangle^2. \quad (8)$$

This quantity was previously investigated in the computational complexity context in [17,20,21,25–28]. As $H(t)$ is a sum over integrals of local operators, the Fubini-Study cost (8) is a linear combination of two-point functions in a state $|\psi(t)\rangle$. Since there is a systematic holographic procedure for calculating two-point functions in any geometric state, the Fubini-Study metric (8) is not only a natural choice from the computational complexity point of view, but also has a natural holographic realization. However, this bulk realization is in general nontrivial: as the states of interest are by construction time-dependent, it requires knowledge of nonequilibrium two-point functions associated to an evolving gravitational background. The dynamics of such two-point functions can be studied, as was done for instance in [29–31], but in general is accessible only via means of numerical holography [32]. This makes the computation of (8) rather challenging to pursue in a generic setup.

In our work we strive for more, namely for obtaining access to such two-point functions just from the knowledge

²In a restricted special case this also applies to the Fubini-Study complexity: for states that are perturbative conformal transformations of the vacuum, the Fubini-Study complexity we are considering here was found to be proportional to a difference in “complexity = volume” between the vacuum and the target state up to the third order in perturbation theory [17,20,21]. This agreement would not hold if one were to use the Fubini-Study line element instead of its square in the definition.

of the geometry itself.³ This turns out to be possible for circuits holographically represented by the pure gravity sector of AdS₃ holography. Such circuits are built from insertions of the energy-momentum tensor in two-dimensional CFT acting on an energy eigenstate or a TFD state. Alternatively, we may view such circuits as realizing a gradual change in the state via conformal transformations. See [20,21,27,41–49] for earlier works on these circuits on, respectively the field theory and gravity sides of the duality. In particular, the authors of [48] studied Fubini-Study cost for circuits implementing global conformal transformations in $d \geq 2$ and derived a bulk dual to the Fubini-Study metric for this particular class of circuits.

Building on previous work [17], in the present paper we map the Fubini-Study distance (8) along the boundary circuit to a geometric quantity in the gravity theory using the AdS/CFT dictionary. From a broader perspective, we thus provide a precise relation between infinitely dimensional complexity geometry associated with the Fubini-Study cost studied in [20,21] and the holographic geometry of AdS universes. The gravity expression we find applies to all asymptotically AdS₃ geometries without matter fields dual to conformal transformations of the vacuum state and excited as well as thermal states. This result opens up the possibility for deriving further gravity duals of quantum information quantities. It can be also thought of as a natural, yet crucial generalization in the context of holographic complexity of the previous AdS/CFT studies of distance measures between states such as the Fisher information metric [45,50–61].

Furthermore, we also investigate which features expected from computational complexity in finite size chaotic systems are reproduced by the Fubini-Study complexity measure that we consider. In the perhaps most interesting case of the time-evolved TFD state, we find a linear growth of complexity, matching the expectations from [4]. To our knowledge, this is the first time that this feature is found in a scenario where both the bulk and boundary sides are under control and the equality of both descriptions is derived from the AdS/CFT dictionary. Moreover, we apply the gravity expression—that we found to be dual to the Fubini-Study distance in bulk geometries without matter fields—to a class of shock wave geometries sourced by sharply concentrated bulk matter. This reproduces a characteristic time delay in the growth of complexity known as the switchback effect [7,62], a further important feature of complexity in finite size systems. However for the states dual to the shock wave geometries, the Fubini-Study distance (8) is by definition constant in

³Obtaining observables just from the geometry itself is possible for one-point functions of local operators [2,3,15,16,33], Wilson loops [34,35] and the fine-grained entropy [36–39]. In contrast, the computation of higher Rényi entropies requires backreaction [40] and hence these entropies are not encoded in the non-backreacted geometry itself.

time and hence cannot show any sign of the switchback effect. Therefore, in this case our new geometric bulk quantity is no longer dual to the Fubini-Study distance.

In summary, we have constructed a gravity observable that satisfies the main features required for a holographic complexity measure—linear growth and the switchback effect—whose field theory dual is known for all geometries without matter fields through a first principles derivation.

The outline of our paper is as follows. We start in Sec. II with a review of the construction from [17] of the bulk dual to a circuit of conformally transformed CFT states. In Sec. III, we construct the bulk dual to the Fubini-Study distance. The Fubini-Study complexity of the time-evolved TFD state is studied in Sec. IV while Sec. V deals with the question whether it can reproduce the switchback effect. We close in Secs. VI and VII with a discussion and outlook. In Appendix A, we comment on the differences between our work and [48]. Appendix B corroborates our results on the switchback effect discussed in Sec. V by studying it in different shock wave geometries.

II. SETUP: HOLOGRAPHIC DUAL TO QUANTUM CIRCUITS

As outlined in the Introduction, studying holographically generated by arbitrarily smeared local operators in holographic QFTs is of key importance for providing a microscopic understanding of holography of complexity. The simplest available setting is the energy-momentum sector of two-dimensional holographic conformal field theories, which generate (in general, local) conformal transformations. In [17], we presented a general prescription for constructing an exact gravity dual for quantum circuits generated by conformal transformations. Here, we briefly review these results, as they allow us to study explicitly the gravity dual to the Fubini-Study cost and, in the eternal black hole geometry, also to the associated complexity.

We consider a two-dimensional CFT in the standard Euclidean framework obtained by analytic continuation $t \rightarrow it$ from Lorentzian signature. In two dimensions, conformal transformations generate two copies of the Virasoro group whose group elements are orientation preserving diffeomorphisms,

$$z \rightarrow f(z), \quad (9)$$

of the complex coordinate $z = t + i\phi$ where t is the time coordinate and $\phi \in [0, 2\pi)$ the angular coordinate. In this setup, the quantum circuit we consider corresponds to a path $f(\tau, z)$ through the space of diffeomorphisms. As a function of the parameter τ , $f(\tau, z)$ determines the conformal transformation that when applied onto the reference state $|\psi(0)\rangle$ yields the state $|\psi(\tau)\rangle$. Infinitesimal changes $f(\tau, z) \rightarrow f(\tau + d\tau, z)$ along the path are generated by [27,41]

$$Q(\tau) = \int_0^{2\pi} \frac{d\phi}{2\pi} \epsilon(\tau, z) T(z) = \sum_{n=-\infty}^{\infty} \epsilon_{-n}(\tau) L_n. \quad (10)$$

Here, $T(z) = \sum_n L_n e^{nz}$ is the energy-momentum tensor with Virasoro generators L_n obeying the venerable Virasoro algebra,

$$[L_n, L_m] = (n - m)L_{n+m} + \frac{c}{12}(n^3 - n)\delta_{n+m,0}, \quad (11)$$

and $\epsilon(\tau, z)$ admits the Fourier expansion $\epsilon(\tau, z) = \sum_n \epsilon_n(\tau) e^{nz}$. The infinitesimal diffeomorphism $z \rightarrow z + \epsilon(\tau, z)$ is related to the path $f(\tau, z)$ by the multiplication law of the Virasoro group, giving

$$\epsilon(\tau, f(\tau, z)) = \frac{d}{d\tau} f(\tau, z). \quad (12)$$

There are two ways to interpret this circuit gravitationally depending on whether the variable τ is taken to be an external auxiliary parameter or identified with the physical time. In the former case, each value of τ is associated to a different bulk geometry where for all τ , the state $|\psi(\tau)\rangle$ lives on the same time slice in physical time (say at $t = 0$)

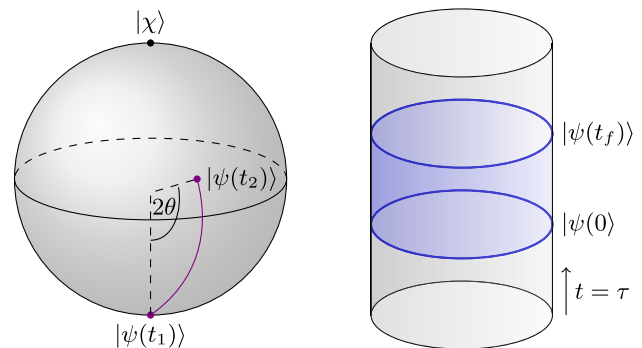


FIG. 1. Illustration of the map between a distance measure in the complexity geometry on the left and a geometric object in the asymptotically AdS spacetime on the right. Any two states $|\psi(t_1)\rangle, |\psi(t_2)\rangle$ can be put on a Bloch sphere spanned by $|\psi(t_1)\rangle$ and an orthogonal state $|\chi\rangle$ obtained by subtracting from $|\psi(t_2)\rangle$ the part parallel to $|\psi(t_1)\rangle$, i.e. $|\psi(t_2)\rangle \propto |\chi\rangle + \langle\psi(t_1)|\psi(t_2)\rangle|\psi(t_1)\rangle$. The geodesic distance for the Fubini-Study metric between $|\psi(t_1)\rangle$ and $|\psi(t_2)\rangle$ is then the angle θ on this Bloch sphere. These two states live on different time slices at the boundary of the same AdS geometry shown on the right-hand side. The infinitesimal distance in the complexity geometry on the left between the states $|\psi(t_1 = t)\rangle$ and $|\psi(t_2 = t + dt)\rangle$ manifests itself as a geometric object in the AdS space on the right. Therefore, the total cost also acquires a geometric dual localized in between the two time slices $t = 0$ and $t = t_f$ in the AdS space. For optimal circuits, this geometric object becomes a gravity dual to the complexity.

on the AdS boundary. For conformal transformations acting on pure states of the CFT, these bulk geometries are Bañados geometries. On the other hand, if the parameter τ is identical to the physical time t , the states $|\psi(\tau)\rangle$ live on different time slices on the boundary of the same asymptotically AdS spacetime (see Fig. 1). In this case, the nontrivial time evolution is generated by turning on a source term for the energy-momentum tensor in the path integral picture. It is the latter picture that we will use in the following.

Let us now describe in more detail how to obtain the correct source term for a given circuit determined by the path $f(t, z)$. As the energy-momentum tensor on the boundary is sourced by the boundary metric $g_{ij}^{(0)}$, we need to consider the CFT on a nontrivial background metric. This background metric is nontrivial but fixed, and thus this procedure does not lead to the introduction of dynamical gravity on the boundary. The exact form of the background metric is determined by demanding that the physical Hamiltonian $H(t)$ and the sum of the left- and right-moving conformal transformation generators $Q(t)$ and $\bar{Q}(t)$ are equal,

$$H(t) = \int d\phi \sqrt{\det(g^{(0)})} T'_t \stackrel{!}{=} Q(t) + \bar{Q}(t). \quad (13)$$

This condition ensures that the sequence of states generated by time-evolution in the background $g_{ij}^{(0)}$ is the same as the sequence of states generated by the path ordered exponential (1) together with its right-moving counterpart.

The solution of (13) is given as follows. At $t < 0$, before the circuit begins acting, the background metric for the CFT is given by $ds_{(0)}^2 = dzd\bar{z}$ and the Hamiltonian is the standard CFT Hamiltonian $H(t) = L_0 + \bar{L}_0$. For $0 \leq t \leq t_f$, the circuit implements non-trivial conformal transformations. In this time range, the boundary metric is given by

$$ds_{(0)}^2 = \left(\frac{\partial f}{\partial z}\right) \left(\frac{\partial \bar{f}}{\partial z}\right) dz^2 + \left(\frac{\partial f}{\partial z}\right) \left(\frac{\partial \bar{f}}{\partial \bar{z}}\right) + \left(\frac{\partial f}{\partial \bar{z}}\right) \left(\frac{\partial \bar{f}}{\partial z}\right) dzd\bar{z} + \left(\frac{\partial f}{\partial \bar{z}}\right) \left(\frac{\partial \bar{f}}{\partial \bar{z}}\right) d\bar{z}^2, \quad 0 \leq t \leq t_f, \quad (14)$$

where the derivatives acting on $f \equiv f(t, z)$ and $\bar{f} \equiv \bar{f}(t, \bar{z})$ in this expression are all nonvanishing because $t = (z + \bar{z})/2$ depends implicitly on z and \bar{z} . Note that the metric in (14) is flat. This property, which is special to two dimensions, means that the nontrivial time-evolution we are after is obtained simply by deforming the timelike

slices on which the states are defined.⁴ Finally, at time $t > t_f$ we have arrived at the target state. In this range of the time coordinate the function $f(t, z) = f(t_f, z)$ is independent of t and the metric (14) reduces to⁵

$$ds_{(0)}^2 = \left(\frac{\partial f(t_f, z)}{\partial z}\right) \left(\frac{\partial \bar{f}(t_f, \bar{z})}{\partial \bar{z}}\right) dzd\bar{z}, \quad t > t_f. \quad (17)$$

Finally, in order to obtain the bulk metric we employ the Fefferman-Graham expansion [63,64],

$$ds^2 = \frac{dr^2}{r^2} + \left(\frac{1}{r^2} g_{ij}^{(0)} + g_{ij}^{(2)} + r^2 g_{ij}^{(4)}\right) dx^i dx^j, \quad (18)$$

where

$$g_{ij}^{(2)} = -\frac{1}{2} R^{(0)} g_{ij}^{(0)} - \frac{6}{c} \langle T_{ij} \rangle \quad \text{and} \\ g_{ij}^{(4)} = \frac{1}{4} (g^{(2)} (g^{(0)})^{-1} g^{(2)})_{ij}. \quad (19)$$

Unlike in higher dimensions, the Fefferman-Graham expansion truncates, and therefore the expression (18) is valid for all r . The energy-momentum tensor expectation values in (19) are determined from the expectation values $\langle T_{ij} \rangle$ in the background $ds_{(0)}^2 = dzd\bar{z}$ by the same coordinate transformation $z \rightarrow f(t, z)$, $\bar{z} \rightarrow \bar{f}(t, \bar{z})$ that leads to the expression (14) for the boundary metric. For example, for

⁴The fact that we can restrict to flat metrics can be justified as follows. An arbitrary curved metric in two dimensions can be written as a Weyl transformation $e^{-2\omega} ds_{(0)}^2$ of a flat metric. Under this transformation, the energy-momentum tensor acquires an additional term which is constant, i.e. proportional to the identity operator,

$$T_{ij} \rightarrow T_{ij} + \frac{c}{6} \left(\partial_i \omega \partial_j \omega - \frac{1}{2} g_{ij}^{(0)} \partial^k \omega \partial_k \omega - \nabla_i^{(0)} \nabla_j^{(0)} \omega + g_{ij}^{(0)} \nabla_k^{(0)} \nabla_k^{(0)} \omega \right). \quad (15)$$

Therefore, also the Hamiltonian $H(t)$ changes by a constant term under this transformation. However, the circuit Hamiltonians $Q(t)$ and $\bar{Q}(t)$ do not include any terms proportional to the identity operator, thereby allowing us to exclude curved background metrics.

⁵It is possible to transform back to a frame in which the metric is $ds_{(0)}^2 = dzd\bar{z}$ by applying a residual flatness preserving Weyl transformation,

$$ds_{(0)}^2 \rightarrow e^{-2\omega} ds_{(0)}^2 = \frac{1}{f'(t_f, F(t_f, f(t, z)))} ds_{(0)}^2, \quad (16)$$

where $f'(t, z)$ denotes the derivative with respect to the second argument. Since this transformation leaves the final state invariant up to an overall phase factor, it is not strictly necessary, and we will omit it in the following.

a sequence of states $|\psi(t)\rangle$ given by conformal transformations of the vacuum state, the expectation values in the background $ds_{(0)}^2 = dzd\bar{z}$ are given by $\langle T_{zz} \rangle = \langle T_{\bar{z}\bar{z}} \rangle = -c/24$, $\langle T_{z\bar{z}} \rangle = 0$ and transform to

$$\begin{aligned}\langle T_{zz} \rangle &= -\frac{c}{24} \left(\left(\frac{\partial f}{\partial z} \right)^2 + \left(\frac{\partial \bar{f}}{\partial \bar{z}} \right)^2 \right), \\ \langle T_{\bar{z}\bar{z}} \rangle &= -\frac{c}{24} \left(\left(\frac{\partial f}{\partial \bar{z}} \right)^2 + \left(\frac{\partial \bar{f}}{\partial z} \right)^2 \right), \\ \langle T_{z\bar{z}} \rangle &= -\frac{c}{24} \left(\left(\frac{\partial f}{\partial z} \right) \left(\frac{\partial f}{\partial \bar{z}} \right) + \left(\frac{\partial \bar{f}}{\partial z} \right) \left(\frac{\partial \bar{f}}{\partial \bar{z}} \right) \right)\end{aligned}\quad (20)$$

in the background (14). This procedure yields a bulk dual to the quantum circuit generated by $Q(t)$ and $\bar{Q}(t)$, in which the entire circuit is encoded in the evolution of a single bulk geometry.

III. HOLOGRAPHIC DUAL TO FUBINI-STUDY DISTANCE

The goal of this section is to derive the gravitational dual to the Fubini-Study distance (5) in the circuit construction described in Sec. II. From a high level point of view, this crucial step provides a bridge between an auxiliary circuit

$$\ell = \log \left[\frac{\sin((f(t_2, z_2) - f(t_1, z_1))/2) \sin((\bar{f}(t_2, \bar{z}_2) - \bar{f}(t_1, \bar{z}_1))/2)}{\epsilon_{UV}^2} \right], \quad (21)$$

where f, \bar{f} parametrize the conformal transformations which define the circuit and ϵ_{UV} is a UV cutoff.

The goal is now to find a relation between the geodesic length ℓ and the two-point function of the Hamiltonian density whose integral gives the Fubini-Study cost function (8). For the trivial circuit $f(t, z) = z$, $\bar{f}(t, \bar{z}) = \bar{z}$, it is easy to express connected two-point correlators of the energy-momentum tensor in terms of ℓ ,

$$\langle T(z_1)T(z_2) \rangle = \frac{c}{32} \frac{1}{\sin((z_1 - z_2)/2)^4} = \frac{c}{2} (\partial_{z_1} \partial_{z_2} \ell)^2. \quad (22)$$

This leads to the following connected two-point function of the Hamiltonian density:

$$\begin{aligned}\langle \mathcal{H}(z_1, \bar{z}_1) \mathcal{H}(z_2, \bar{z}_2) \rangle &= \langle T(z_1)T(z_2) \rangle + \langle \bar{T}(\bar{z}_1)\bar{T}(\bar{z}_2) \rangle \\ &= \frac{c}{2} [(\partial_{z_1} \partial_{z_2} \ell)^2 + (\partial_{\bar{z}_1} \partial_{\bar{z}_2} \ell)^2] \\ &= \frac{c}{4} [(\partial_{\phi_1} \partial_{t_2} \ell)(\partial_{t_1} \partial_{\phi_2} \ell) \\ &\quad + (\partial_{\phi_1} \partial_{\phi_2} \ell)(\partial_{t_1} \partial_{t_2} \ell)].\end{aligned}\quad (23)$$

For our circuit we have to allow arbitrary f and \bar{f} . In this case, after some algebra we find the following relation

geometry defined in terms of the boundary quantities and the bulk geometry of AdS.

We will construct this gravity dual using techniques inspired by mathematical tools from integral geometry known under the name of kinematic space [65]. In our setup the kinematic space is the space of all geodesics anchored on the asymptotic boundary.⁶ This auxiliary space has been used previously to reformulate geometric objects in asymptotically AdS₃ spaces as functionals on the kinematic space; see e.g. [66–77]. In particular, complexity measures outside the realm of complexity geometry have been explored in the context of the kinematic space in [78,79]. By the Ryu-Takayanagi formula, which associates the length of the geodesics in the kinematic space with the CFT entanglement entropy, the kinematic space formulation of the problem allows a derivation of duals to bulk geometric objects in terms of boundary entanglement data. Here, we will do the reverse: we will use the kinematic space to map the Fubini-Study cost function (5)—a boundary quantity—to a geometric object in the bulk defined by its formulation as a kinematic space functional.

Let us first describe the kinematic space in more detail. Each geodesic is specified by its two end points (z_1, \bar{z}_1) and (z_2, \bar{z}_2) . The length of this geodesic in our geometry dual to a quantum circuit is given by

between the connected two-point function of the Hamiltonian density \mathcal{H} and the geodesic length ℓ :

$$\begin{aligned}\sqrt{g_{(0)}(t_1, \phi_1)} \sqrt{g_{(0)}(t_2, \phi_2)} \langle \mathcal{H}(t_1, \phi_1) \mathcal{H}(t_2, \phi_2) \rangle \\ = \partial_{\phi_1} f_1 \partial_{t_1} f_1 \partial_{\phi_2} f_2 \partial_{t_2} f_2 \langle T(f_1)T(f_2) \rangle \\ + \partial_{\phi_1} \bar{f}_1 \partial_{t_1} \bar{f}_1 \partial_{\phi_2} \bar{f}_2 \partial_{t_2} \bar{f}_2 \langle \bar{T}(\bar{f}_1)\bar{T}(\bar{f}_2) \rangle = \mathcal{F}_{\text{bulk}},\end{aligned}\quad (24)$$

where

$$\begin{aligned}\mathcal{F}_{\text{bulk}} = \frac{c}{4} \left[(\partial_{\phi_1} \partial_{\phi_2} \ell)(\partial_{t_1} \partial_{t_2} \ell) + (\partial_{\phi_1} \partial_{t_2} \ell)(\partial_{t_1} \partial_{\phi_2} \ell) \right. \\ \left. - \frac{1}{2} g_{t_1 \phi_1}^{(0)} g_{t_2 \phi_2}^{(0)} g_{(0)}^{ij}(t_1, \phi_1) g_{(0)}^{kl}(t_2, \phi_2) (\partial_i \partial_k \ell)(\partial_j \partial_l \ell) \right].\end{aligned}\quad (25)$$

Therefore, we have found a bulk dual to the Fubini-Study cost function,

⁶Note that this includes winding geodesics if the spacetime has nontrivial topology; see Fig. 2.

$$\begin{aligned}
 F_{\text{FS}}(t) &= \int d\phi_1 \int d\phi_2 \sqrt{g_{(0)}(t, \phi_1)} \\
 &\quad \times \sqrt{g_{(0)}(t, \phi_2)} \langle \mathcal{H}(t, \phi_1) \mathcal{H}(t, \phi_2) \rangle \\
 &= F_{\text{bulk}}(t) = \int d\phi_1 \int d\phi_2 \mathcal{F}_{\text{bulk}}, \quad (26)
 \end{aligned}$$

expressed in terms of geodesic lengths. This mapping between a natural measure of distance between states and a purely geometric object in the bulk is our first main technical result. As (26) was derived from the AdS/CFT dictionary, it is valid for any quantum circuit built out of conformal transformations. Note that despite the geodesic length ℓ being UV divergent, (26) is UV finite. This is to be expected, since applications of exponents of smeared local operators (in our case, the energy-momentum tensor) are not expected to alter the ultraviolet behavior of the states. Indeed, the Fubini-Study distance was shown in [20,21] to exhibit UV finiteness for the circuits used here.⁷

Interestingly, the volume V of a constant time slice of pure AdS₃ from the ‘‘complexity = volume’’ proposal can be also obtained from the kinematic space formulation in the trivial circuit $f(t, z) = z$, $\bar{f}(t, \bar{z}) = \bar{z}$. It is given by a formula similar to (26) [75,76],

$$V = \int d\phi d\rho \sqrt{g_{\text{ind}}(\phi, \rho)} \propto \int d\phi_1 \int d\phi_2 \ell \partial_{\phi_1} \partial_{\phi_2} \ell, \quad (27)$$

where g_{ind} is the induced metric on the constant time slice in the bulk and ρ the AdS₃ radial coordinate. Both (27) and (26) are quadratic in the geodesic length ℓ but differ in the structure of derivatives applied to ℓ . Because ℓ appears without a derivative in (27), the volume is UV divergent.

A. Conical defects

In fact, while we have derived the formula (26) only for circuits comprising states that are conformal transformations

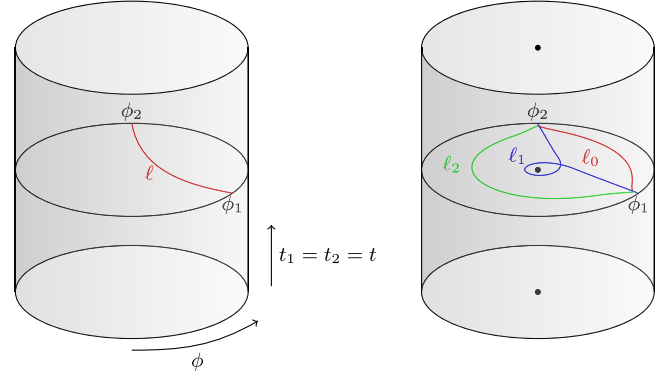


FIG. 2. Boundary anchored geodesics making up the kinematic space for the AdS₃ geometry dual to a conformally transformed vacuum state on the left and the \mathbb{Z}_3 conical defect dual to an excited state on the right.

of the vacuum state, it applies to a much wider set of cases. In particular, we find that (26) also holds for conformal transformations of primary states with conformal weight $h = \frac{c}{24}(1 - 1/n^2)$ where $n \in \mathbb{N}$. For excited primary states, the connected two-point function of the energy-momentum tensor is given by

$$\begin{aligned}
 \langle h|T(z_1)T(z_2)|h \rangle &= \frac{c}{32} \frac{1}{\sin^2((z_1 - z_2)/2)^4} \\
 &\quad - \frac{h}{2} \frac{1}{\sin^2((z_1 - z_2)/2)^2}. \quad (28)
 \end{aligned}$$

These states are dual to conical defects arising from a \mathbb{Z}_n identification of pure AdS₃. In this spacetime, there are n geodesics connecting two boundary points (t_1, ϕ_1) , (t_2, ϕ_2) with winding numbers $w = 0, \dots, n-1$ (see Fig. 2) and length,

$$\ell_w = \log \left[\frac{\sin((f(t_2, z_2) - f(t_1, z_1) + 2\pi w)/2n) \sin((\bar{f}(t_2, \bar{z}_2) - \bar{f}(t_1, \bar{z}_1) - 2\pi w)/2n)}{\epsilon_{\text{UV}}^2} \right], \quad (29)$$

Therefore, the kinematic space consists of n sectors with fixed winding number w and to obtain a bulk dual to the connected two-point function of the Hamiltonian density, we have to sum over all w ,

⁷To be precise, it is necessary to choose a regularization procedure for the integral around the point $\phi_1 = \phi_2$ where the two energy-momentum tensor insertions collide [20,21]. This regularization is implicit in writing the Fubini-Study distance as the integral over local operators and does not affect the final result.

$$\begin{aligned}
 &\sqrt{g_{(0)}(t_1, \phi_1)} \sqrt{g_{(0)}(t_2, \phi_2)} \langle h|\mathcal{H}(t_1, \phi_1)\mathcal{H}(t_2, \phi_2)|h \rangle \\
 &= \partial_{\phi_1} f_1 \partial_{t_1} f_1 \partial_{\phi_2} f_2 \partial_{t_2} f_2 \langle h|T(f_1)T(f_2)|h \rangle + (c.c) \\
 &= \sum_{w=0}^{n-1} \frac{c}{4} \left[(\partial_{\phi_1} \partial_{\phi_2} \ell_w)(\partial_{t_1} \partial_{t_2} \ell_w) + (\partial_{\phi_1} \partial_{t_2} \ell_w)(\partial_{t_1} \partial_{\phi_2} \ell_w) \right. \\
 &\quad \left. - \frac{1}{2} g_{t_1 \phi_1}^{(0)} g_{t_2 \phi_2}^{(0)} g_{(0)}^{j_1 j_1} g_{(0)}^{k_2 l_2} (\partial_{i_1} \partial_{k_2} \ell_w)(\partial_{j_1} \partial_{l_2} \ell_w) \right]. \quad (30)
 \end{aligned}$$

Inserting this into (26) yields again a geometric expression for the Fubini-Study cost function (8). This determines the

gravity dual to the Fubini-Study distance for any two pure states related by conformal transformations (i.e. any two states in the same Verma module).

B. BTZ black holes

Apart from conical defects, the expression (26) also correctly reproduces the connected two-point function of the Hamiltonian in a thermal state dual to a BTZ black hole or the TFD state,

$$|\text{TFD}(t)\rangle = \frac{1}{\sqrt{Z(\beta)}} \sum_n e^{-iE_n t} e^{-\beta E_n/2} |E_n\rangle_L |E_n\rangle_R, \quad (31)$$

dual to the two-sided BTZ geometry, where the sum runs over all energy eigenstates. In this case, there are multiple geodesics to consider. The length of a geodesic stretching between two-points on the asymptotic boundary of the one-sided BTZ black hole is given by

$$\ell = \log \left[\frac{\cosh(2\pi(\phi_1 - \phi_2)/\beta) - \cosh(2\pi(t_1 - t_2)/\beta)}{\epsilon_{\text{UV}}} \right], \quad (32)$$

while geodesics between two different asymptotic boundaries in the maximally extended two-sided BTZ geometry have length,

$$\ell = \log \left[\frac{\cosh(2\pi(\phi_1 - \phi_2)/\beta) + \cosh(2\pi(t_1 + t_2)/\beta)}{\epsilon_{\text{UV}}} \right]. \quad (33)$$

For geodesics with winding numbers, simply set $\phi_1 - \phi_2 \rightarrow \phi_1 - \phi_2 + 2\pi w$. Applying (24) and (25), integrating over ϕ_1 and ϕ_2 as well as summing over all possible winding numbers⁸ leads also in this case to a result proportional to the thermal two-point function,

$$\langle H^2 \rangle_\beta - \langle H \rangle_\beta^2 = \frac{\partial_\beta^2 Z(\beta)}{Z(\beta)} - \left(\frac{\partial_\beta Z(\beta)}{Z(\beta)} \right)^2 = \frac{2c\pi^2}{3\beta^3}, \quad (34)$$

where $Z(\beta) = \text{Tr}[e^{-\beta H}] = \exp(\frac{c}{12} \frac{4\pi^2}{\beta})$ is the thermal partition function. For the two-sided black hole, the Hamiltonian $H = H_L + H_R$ is the sum of the two Hamiltonians on the left and right asymptotic boundaries and its connected two-point function in the TFD state is given by four times the result of (34). In the bulk, these four contributions come from the four possibilities of placing boundary points (ϕ_1, t_1) , (ϕ_2, t_2) on the two asymptotic boundaries.

⁸The sum over winding numbers is equivalent to integrating $\chi = (\phi_1 + \phi_2)/2$ from 0 to 2π and $\psi = (\phi_1 - \phi_2)/2$ from 0 to ∞ .

We note two small subtleties concerning this result. First, in the case where the integral in (26) runs over the end points of geodesics on the same asymptotic boundary, the integral is formally divergent due to infinities at colliding operator insertion points where $\phi_1 = \phi_2$. A consistent result is obtained through regularization. By restricting $\phi_1 - \phi_2$ to be greater than some value $\tilde{\epsilon}$ we obtain a result where the two-point function of the Hamiltonian emerges at order $O(\tilde{\epsilon}^0)$. Second, in the case where the integral runs over geodesic lengths on different asymptotic boundaries, the time derivatives in (25) have to be taken with respect to the Killing time which is given by t_1 , respectively $-t_2$, on the left, respectively right, asymptotic boundary in order to obtain the correct sign.

In summary, we have found a geometric dual, expressed in terms of geodesic lengths, to the Fubini-Study distance between two states related by infinitesimal time-evolution. This expression applies to all asymptotically AdS₃ spacetimes without bulk matter fields, i.e. Bañados geometries corresponding to conformal transformations of the vacuum state as well as excited primary states and the BTZ black hole corresponding to a thermal state. This maps a cost function of a field theory complexity measure into a purely geometric quantity in the dual field theory, opening the door to studying gravity duals to computational complexity from first principles.

IV. FROM COST TO COMPLEXITY

So far, we have discussed the map between the boundary cost and bulk geometry. With complexity arising from the optimization of the cost, as encapsulated by Eq. (2), in the present section we want to apply our framework to study bulk complexity completely *ab initio*.

The main question we are aiming to answer is the following. It has been conjectured that the computational complexity in quantum systems which describe AdS black holes evolves universally (i.e. for any reasonable definition of complexity) in a particular way with time. It is supposed to increase linearly until an exponentially long timescale in the black hole entropy S , saturates over a duration of a doubly exponentially long timescale until it decreases again at the quantum recurrence time t_{rec} and the process starts anew [4,7,80,81].⁹ We illustrate this expectation in Fig. 3. Our goal for this section is to study which of these features can be reproduced in our approach.

To answer this question, let us first compute the total cost,

$$F_{\text{FS,tot}}(t) = \int_0^t dt' F_{\text{FS}}(t') \quad (35)$$

⁹See also [82,83] for a proof for randomized quantum circuits with a finite number of qubits and [28,84] for a bulk quantum generalization of the ‘‘complexity = volume’’ proposal that exhibits a plateau at very late times.

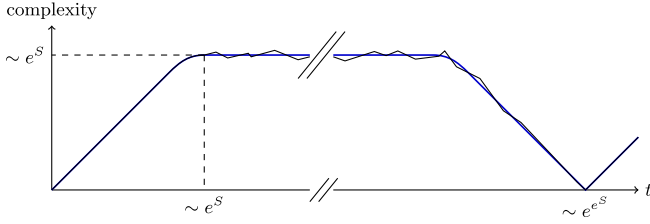


FIG. 3. Time evolution of computational complexity as conjectured by [4].

for a particular circuit that computes the time-evolved TFD state $|\text{TFD}(t)\rangle$ dual to the BTZ black hole in question, without minimizing over different circuits to obtain the complexity. The results for $F_{\text{FS,tot}}$ then provide an upper bound for the complexity. There is one particular circuit for which this is particularly easy to do this and that is the time evolution of the BTZ black hole itself where $|\text{TFD}(t)\rangle$ is created simply by ordinary time evolution with $H = H_L + H_R$ and $H_{L,R} = L_0 + \bar{L}_0$ from the reference state $|\text{TFD}(0)\rangle$. In that case we indeed find a linear increase with t in $F_{\text{FS,tot}}(t)$ due to $F_{\text{FS}}(t)$ being constant in t . Therefore, if the conjecture on the linear increase of complexity is true, then the optimal circuit for constructing the time-evolved TFD state is not far away from ordinary time evolution for less than exponential times.

Similar arguments lead to the dip at the recurrence time. By also allowing circuits which time evolve reversely (i.e. evolution with $-H$ instead of H) it is obvious that the complexity is upper bounded by

$$C_{\text{FS}}(t) \leq \min\left(\int_0^t dt' F_{\text{FS}}(t'), \int_t^{t_{\text{rec}}} dt' F_{\text{FS}}(t')\right), \quad (36)$$

and therefore must decrease to zero again at $t = t_{\text{rec}}$.

To show that ordinary time evolution is indeed optimal, we now optimize the total cost over all circuits that connect $|\text{TFD}(0)\rangle$ with $|\text{TFD}(t)\rangle$ via applying conformal transformations,

$$C_{\text{FS}}(t) = \min F_{\text{FS,tot}}(t). \quad (37)$$

The minimization procedure proceeds by performing a variation of $F_{\text{FS,tot}}(t)$ with respect to $f(t, z)$ and solving the resulting equations of motion to determine the path $f(t, z)$ of least total cost. For simplicity, we restrict to conformal transformations acting only on one boundary of the wormhole.¹⁰

The Fubini-Study cost function in this situation of interest is given by

¹⁰Note that coupling the both boundaries/the both underlying quantum field theories, as, for example, in [23,85], goes significantly beyond the algebraic setup of ours.

$$\begin{aligned} F_{\text{FS}}(t) &= \langle \psi(t) | Q(t)^2 | \psi(t) \rangle - \langle \psi(t) | Q(t) | \psi(t) \rangle^2 \\ &= \langle \text{TFD}(0) | \tilde{Q}(t)^2 | \text{TFD}(0) \rangle \\ &\quad - \langle \text{TFD}(0) | \tilde{Q}(t) | \text{TFD}(0) \rangle^2. \end{aligned} \quad (38)$$

Here, the circuit Hamiltonian $Q(t)$ is defined in (10) while $\tilde{Q}(t)$ is its conformal transformation defined by letting the path ordered exponential from (1) act on $Q(t)$ instead of $|\text{TFD}(0)\rangle$ in (38). From the well-known transformation law of the stress-energy tensor, $\tilde{Q}(t)$ can be written as

$$\tilde{Q}(t) = \int d\phi \left(1 + \frac{\dot{f}(t, z)}{f'(t, z)} \right) \left[T(z) - \frac{c}{12} \{f, z\} \right], \quad (39)$$

using $\epsilon(t, z) = \dot{f}(t, F(t, z)) + f'(t, F(t, z))$ from (12). The notation is such that $F(t, z)$ is the inverse of $f(t, z)$, i.e. $f(t, F(t, z)) = z$, while \dot{f} is the derivative with respect to the first argument of f and f' the one with respect to the second argument. The thermal two-point function of the energy-momentum tensor can be obtained by the conformal Ward identity [86],

$$\begin{aligned} &\langle \text{TFD}(0) | T(z_1) T(z_2) | \text{TFD}(0) \rangle \\ &= \frac{c}{24} \wp'' \left(\frac{z_1 - z_2}{2\pi} \right) + 2 \frac{2\pi i \partial_\tau Z(\tau)}{Z(\tau)} \left(\wp \left(\frac{z_1 - z_2}{2\pi} \right) + 2\eta_1 \right) \\ &\quad + \frac{(2\pi i \partial_\tau)^2 Z(\tau)}{Z(\tau)} - \left(\frac{2\pi i \partial_\tau Z(\tau)}{Z(\tau)} \right)^2, \end{aligned} \quad (40)$$

where $Z(\tau)$ is the (holomorphic part of) the partition function and $\wp(z)$ denotes the Weierstraß elliptic function with associated parameter η_1 . From periodicity in ϕ , it is clear that the Fubini-Study cost must be of the form,

$$F_{\text{FS}} = \sum_{n \geq 0} \alpha_n \gamma_n \gamma_{-n}, \quad (41)$$

where γ_n are the Fourier coefficients of $\gamma = 1 + \dot{f}/f'$. The α_n prefactors are non-negative since F_{FS} is a positive quantity (if α_m were negative for some $m \geq 0$, F_{FS} could become negative as well when $\gamma_m \gg \gamma_{n \neq m}$). The explicit form of α_n can be derived from (40),¹¹ but we will not need it and therefore leave α_n as an unspecified non-negative number in the following discussion.

¹¹For completeness, we note that the ϕ integrals which have to be evaluated in order to compute α_n need to be regularized due to singularities of the two-point function (40) at coincident insertion points $z_1 = z_2$. This can be achieved for instance using differential regularization as in [20]. By writing $\wp((z_1 - z_2)/2) + 2\eta_1 = 2\pi^2 \sum_{m \in \mathbb{Z}} \partial_{\phi_1} \partial_{\phi_2} \log \sinh^2((z_1 - z_2 + 2\pi i m \tau)/2)$ and shifting the $\partial_{\phi_1} \partial_{\phi_2}$ derivatives onto the γ prefactors using partial integration while neglecting the boundary terms, the integral is well-defined, and it can be explicitly seen that α_n is non-negative.

Then, inserting (41) into (35) and varying with respect to f_n , the Fourier coefficients of f , determines the optimal path with minimum total cost. To solve the resulting equations of motion we expand in a perturbation parameter σ , $f(t, z) = z + \sigma f^{(1)}(t, z) + \sigma^2 f^{(2)}(t, z) + O(\sigma^3)$. Written in a polar decomposition for the Fourier coefficients $f_n^{(k)}(t) = |f_n^{(k)}(t)| e^{i\theta_n^{(k)}(t)}$, this gives to leading order in σ the equations of motion,

$$\begin{aligned} \ddot{f}_0^{(1)} &= 0 \quad \text{for } n = 0 \\ \alpha_0 n \partial_t |f_n^{(1)}|^2 &= 0, \quad \alpha_n |\dot{f}_n^{(1)}| + 2\alpha_0 n \dot{\theta}_n^{(1)} |f_n^{(1)}| = 0 \\ &\text{for } n > 0. \end{aligned} \quad (42)$$

For the target state $|\text{TFD}(t_f)\rangle$, the boundary conditions for these equations are $f(t=0) = f(t=t_f) = z$. Therefore, we find from (42) that $f_n^{(1)} = 0$ for all n . As the first order contribution in σ to $f(t, z)$ vanishes, we deduce that the second order contribution vanishes as well (simply replace $\sigma^2 \rightarrow \sigma$ to get the same equation of motion for $f_n^{(2)}$ as for $f_n^{(1)}$). Hence, order by order in perturbation theory we find that time evolution by nontrivial conformal transformations is more expensive in our setup than ordinary time evolution with $H = L_0 + \bar{L}_0$. Thus, the computational complexity increases or decreases linearly in the regime where perturbation theory is applicable, i.e. at times close to zero or close to a multiple of the recurrence time.

In the complexity geometry picture of [14], contributions which might be invisible in perturbation theory can in particular appear at conjugate points in the complexity geometry. In previous studies of computational complexity in chaotic systems, the appearance of conjugate points has lead to a saturation of computational complexity; see e.g. [87–89]. In our setup, the notion of conjugate points on a geodesic in a Finsler geometry as used by [14] is not applicable because the squared Fubini-Study distance is positively homogeneous of degree two under $H \rightarrow \alpha H$ instead of degree one as required for a Finsler metric. Nevertheless, similar effects which our perturbative calculation cannot capture might still lead to a saturation in our case.

V. THE FUBINI-STUDY COST FUNCTION AND THE SWITCHBACK EFFECT

Given that the bulk dual to the Fubini-Study cost derived in Sec. III in the BTZ geometry correctly reproduces the thermal two-point function, we now study what happens if bulk matter fields enter the picture. In particular, we investigate BTZ geometries perturbed by adding shock waves. In this situation computational complexity shows a striking time dependence where an exponential growth regime turns into a linear one at the scrambling time, a phenomenon known as the switchback effect [7,62].

We find that the geometric expression F_{bulk} from Eq. (25), which we found to be dual to the Fubini-Study distance, is sensitive to the switchback effect but that the Fubini-Study cost is not. This shows that the equality between the Fubini-Study distance and F_{bulk} is not applicable to geometries sourced by bulk matter fields (and indeed there is no reason to expect it to). Nevertheless, the fact that F_{bulk} can probe the switchback effect implies that this quantity shows the features generally expected from a cost function for a holographic complexity measure [11,12]: linear growth at late times in the BTZ wormhole geometry and an imprint of the switchback effect [4,7,62].

Let us now briefly review the switchback effect on the field theory side. In the computational complexity setup, the perturbation generating the shock wave in the dual bulk picture is implemented by applying a precursor operator which in the *Schrödinger picture* is given by $U^\dagger(t_W) W U(t_W)$. The standard, discrete gate-counting complexity of this operator on its own can be estimated by a simple infection model [7,81]. In this model, the operator W acts on a single qubit and is counted as a single gate. The complexity of the precursor $U^\dagger(t_W) W U(t_W)$ is then given by one plus the number of gates in $U^\dagger(t_W)$ and $U(t_W)$ minus the number of gates that cancel between $U^\dagger(t_W)$ and $U(t_W)$. How many such cancellations occur is determined by an infection model: by acting with W on a qubit, this qubit becomes infected and the infection spreads throughout the quantum system when an infected qubit couples to a noninfected one by two- or more qubit gates in $U(t_W)$. Gates inside $U(t_W)$ and $U^\dagger(t_W)$ cancel if they act on noninfected qubits. This leads to a complexity of the precursor operator given by [7,81]

$$C \propto K \log(1 + e^{\frac{2\pi}{\beta}(t_W - t_*)}), \quad (43)$$

where K is the number of qubits and t_* is the scrambling time, given by $t_* = \frac{\beta}{2\pi} \log c$ in two-dimensional CFTs [90]. There is a characteristic time delay in the complexity growth: for $W \neq \mathbf{1}$ there is first an exponential increase in t_W for small t_W followed by a linear growth regime.¹²

In the context of two-dimensional conformal field theories, the operator W is taken to be a heavy primary operator whose insertion at $t = t_W \rightarrow -\infty$ leads to a null shock wave propagating along the horizon [90]. On the gravity side, the computational complexity of the precursor is then estimated by applying one of the holographic

¹²It is important to note that this behavior is observed for the t_W dependence, the parameter of the precursor. The model does not capture subsequent time evolution $U(t)|\psi(0)\rangle = U(t)U^\dagger(t_W)WU(t_W)|\text{TFD}(0)\rangle$ occurring after the precursor has been applied onto the TFD state, and hence the complexity is only the complexity of the precursor operator itself.

complexity proposals¹³ which shows the same time-evolution behavior (43) as obtained from the infection models described above. This has been derived for the “complexity = volume” proposal in [7] and for the “complexity = action” proposal in [8,9]. This property also holds by construction for the infinite families of holographic complexity measures proposed in [11,12], as it is one of their two defining features.

However, for the field theory quantity that we are considering—the Fubini-Study cost (8) and its time integral (35)—it is clear that (43) cannot be reproduced. It is easy to see¹⁴ that the Fubini-Study distance between the state $|\psi\rangle = U^\dagger(t_W)WU(t_W)|\text{TFD}(0)\rangle$ and the state $e^{iHdt}|\psi\rangle$ is independent of t_W . In fact, this argument showing that expectation values $\langle\psi|\mathcal{O}|\psi\rangle$ are independent of t_W holds for any operator \mathcal{O} that is diagonal in the energy eigenbasis. The independence of the Fubini-Study distance of t_W should not come as a surprise, as the switchback effect is expected to follow from locality, whereas the Fubini-Study cost does not account for it explicitly.¹⁵

Nevertheless, the geometric expression F_{bulk} obtained in Sec. III—which for bulk geometries without matter fields is equal to the Fubini-Study cost function—reproduces the switchback effect as we will show below. This makes clear that this expression is not dual to the Fubini-Study cost function for the perturbed TFD states.

We now come to the gravitational calculation of F_{bulk} in the shock wave geometries. The shock wave geometries we consider are given by portions of BTZ geometries glued together along null surfaces [91]. For a shock wave moving from the bottom left to the top right in the Penrose diagram, in Kruskal coordinates a point $(u = 0, v, \phi)$ on one side is identified with $(u = 0, v + h(\phi), \phi)$ on the other side where the displacement $h(\phi)$ depends on the exact form of the bulk matter concentration that sources the shock wave. We will consider bulk matter that is concentrated along the horizon at $u = 0$ in Kruskal coordinates as well as localized at $\phi = \hat{\phi}$ in the angular direction similar to the setup in [92]. The periodicity $\phi \sim \phi + 2\pi$ requires the bulk energy-momentum tensor to be given by

$$T_{uu} = \frac{\alpha}{2\pi G_N} \sum_{n \in \mathbb{Z}} \delta(u) \delta(\phi - \hat{\phi} + 2\pi n). \quad (44)$$

¹³At $t = 0$ in order to capture the complexity of the precursor and not any subsequent time evolution.

¹⁴Let the TFD state be given by $|\text{TFD}\rangle = \frac{1}{\sqrt{Z(\beta)}} \sum_n e^{-\beta E_n/2} |E_n\rangle_L |E_n\rangle_R$ and expand the operator W in energy eigenstates, $W = \sum_{n,m} W_{nm} |E_n\rangle_L \langle E_m|_L \times \mathbf{1}_R$. Then, by an elementary calculation we see that the expectation values $\langle\psi|H|\psi\rangle$ and $\langle\psi|H^2|\psi\rangle$ are independent of t_W , and, via (8), it settles the point.

¹⁵We thank Qi-Feng Wu for pointing this out.

while the other components of $T_{\mu\nu}$ vanish. The parameter,

$$\alpha = 2 \exp\left(-\frac{2\pi}{\beta}(t_W - t_*)\right), \quad (45)$$

determines the strength of the shock [7]. Solving Einstein’s equations gives a metric of the form,

$$ds^2 = -\frac{4}{(1+uv)^2} dudv + r_H^2 \frac{(1-uv)^2}{(1+uv)^2} d\phi^2 + 4\delta(u)h(\phi)du^2, \quad (46)$$

where the displacement along the horizon at $u = 0$ is given by

$$v \rightarrow v + h(\phi) \quad \text{with} \\ h(\phi) = \alpha \frac{\cosh(r_H(|\phi - \hat{\phi}| - \pi(2n-1)))}{\sinh(r_H\pi)}, \\ \pi(n-1) \leq |\phi - \hat{\phi}| \leq \pi n. \quad (47)$$

Here, $r_H = \frac{2\pi}{\beta}$ is the horizon radius. For a shock wave moving in the opposite direction (bottom right to top left), the gluing condition is $(u - h(\phi), v = 0, \phi) \sim (u, v = 0, \phi)$ and $\alpha = 2 \exp(-\frac{2\pi}{\beta}(t_W + t_*))$.

In order to check if the quantity F_{bulk} from (26) can reproduce (43), we first have to derive the geodesic lengths between opposite asymptotic boundaries of the shock wave geometries. This is easy to do with a recipe from [91]. All asymptotically AdS₃ geometries can be embedded into a four-dimensional embedding space $\mathbf{R}^{2,2}$. The geodesic length ℓ between two points (T_1, T_2, X_1, X_2) and (T'_1, T'_2, X'_1, X'_2) in the embedding space is given by

$$\cosh(\ell) = T_1 T'_1 + T_2 T'_2 - X_1 X'_1 - X_2 X'_2. \quad (48)$$

The embedding space coordinates are related to the Kruskal,

$$ds^2 = \frac{-4dudv + r_H^2(1-uv)^2 d\phi^2}{(1+uv)^2}, \quad (49)$$

and BTZ coordinates,

$$ds^2 = -(r^2 - r_H^2)dt^2 + \frac{dr^2}{r^2 - r_H^2} + r^2 d\phi^2, \quad (50)$$

by

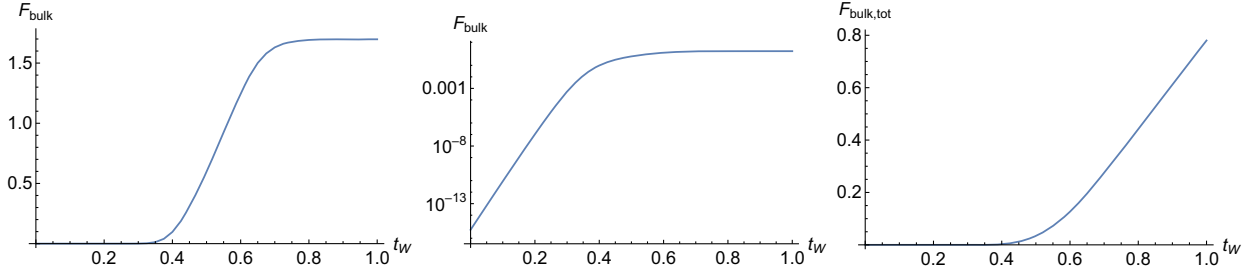


FIG. 4. Left and center: the bulk cost function F_{bulk} plotted over t_W in the localized shock wave geometry with compact horizon on a linear resp. logarithmic scale. Right: the corresponding total cost $F_{\text{bulk,tot}}$ (the t_W integral of F_{bulk}). The plots match perfectly with the expectation from the infection models that the exponential increase, which is clearly visible in the log-scale plot in the center, turns into a linear increase at the scrambling time. All plots are evaluated for $t_* = 0.5$ and $\beta = 1/4$.

$$\begin{aligned}
 T_1 &= \frac{v+u}{1+uv} = \frac{\sqrt{r^2 - r_H^2}}{r_H} \sinh(r_H t), \\
 T_2 &= \frac{1-uv}{1+uv} \cosh(r_H \phi) = \frac{r}{r_H} \cosh(r_H \phi), \\
 X_1 &= \frac{v-u}{1+uv} = \frac{\sqrt{r^2 - r_H^2}}{r_H} \cosh(r_H t), \\
 X_2 &= \frac{1-uv}{1+uv} \sinh(r_H \phi) = \frac{r}{r_H} \sinh(r_H \phi). \quad (51)
 \end{aligned}$$

The length of a geodesic in the shock wave geometry is then obtained by adding together the length ℓ_1 of a geodesic running from the right boundary to a point ($u = 0, v = v_s, \phi = \phi_s$) on the horizon with the length ℓ_2 of a geodesic running from ($u = 0, v = v_s + h(\phi_s), \phi = \phi_s$) to the left boundary. The total geodesic length is given by $\ell = \ell_1 + \ell_2$ subject to the minimality conditions,

$$\partial_{v_s} \ell = \partial_{\phi_s} \ell = 0. \quad (52)$$

Solving these equations yields

$$\begin{aligned}
 \ell &= \log \left[\frac{1}{2} \left(\cosh(2r_H \bar{t}) + \cosh(2r_H \Delta \phi) \right. \right. \\
 &\quad + \alpha e^{r_H t_1} \cosh(r_H (\phi_2 - \hat{\phi} - (2n-1)\pi)) \\
 &\quad + \alpha e^{-r_H t_2} \cosh(r_H (\phi_1 - \hat{\phi} - (2n-1)\pi)) \\
 &\quad \left. \left. + \frac{1}{2} \alpha^2 e^{2r_H \Delta t} \right) \right], \quad \Delta \phi_{n-1} \lesseqgtr \Delta \phi \lesseqgtr \Delta \phi_n, \quad (53)
 \end{aligned}$$

where $\phi_{1,2} = \bar{\phi} \pm \Delta \phi$, $t_{1,2} = \bar{t} \pm \Delta t$ and $\Delta \phi_n = \frac{1}{2} \log \left[\frac{\sinh(r_H (\bar{t} + (\bar{\phi} - \hat{\phi} - 2\pi n)))}{\sinh(r_H (\bar{t} - (\bar{\phi} - \hat{\phi} - 2\pi n)))} \right]$ for $1 \leq n \leq \lfloor \frac{|\bar{t} + \bar{\phi} - \hat{\phi}|}{2\pi} \rfloor$. For the \lesseqgtr comparison, the upper comparator is chosen for $\bar{t} > 0$ and the lower one for $\bar{t} < 0$.

We then insert this geodesic length into (26) and evaluate the resulting expressions numerically. The results for geodesics anchored at $t = 0$ show that there is a time delay in

t_W before F_{bulk} saturates to the value of the Fubini-Study distance in the TFD state (see Fig. 4). Consequently, the total cost (35) increases linearly with a time delay. This matches perfectly with the expectations from the simple infection models for computational complexity described above: the total cost first starts from zero, then increases exponentially until the scrambling time and linearly afterwards.¹⁶ Up to numerical errors and an overall prefactor of t_W and t_* which is not fixed in the infection models (one may always rescale the time which it takes for one layer of the circuit to act in the infection model by a constant), the total cost is given by the right hand side of (43) when the number of qubits K is identified with the central charge c , as in [81].

In Appendix B, we study further shock wave geometries with noncompact horizons and delocalized matter concentrations where we again qualitatively reproduce the switchback effect from the geometric expression F_{bulk} although the matching to the expectations from the infection model is not as good as above.

VI. DISCUSSION

Providing a more microscopic picture of optimal state preparation in holography, based on quantum field theory, is an important open research question that has not been yet satisfactorily answered for any of the existing holographic complexity proposals. Arguably, our best bet for a definition of complexity in quantum field theory stems from [14] and is based on minimizing cost functionals for continuous quantum circuits (1). Therefore, it is natural to expect that

¹⁶Note that here we are comparing a total cost on the gravity side with expectations about complexity (the minimal total cost). Therefore the match is not obvious not only because the cost function we use on the gravity side might not be sensitive to the switchback effect but also because this effect might only appear after optimizing. However, we have already determined in Sec. IV that complexity and total cost are the same in the BTZ black hole (ordinary time evolution is the optimal path), and therefore it is reasonable to expect that the same happens in the shock wave geometries.

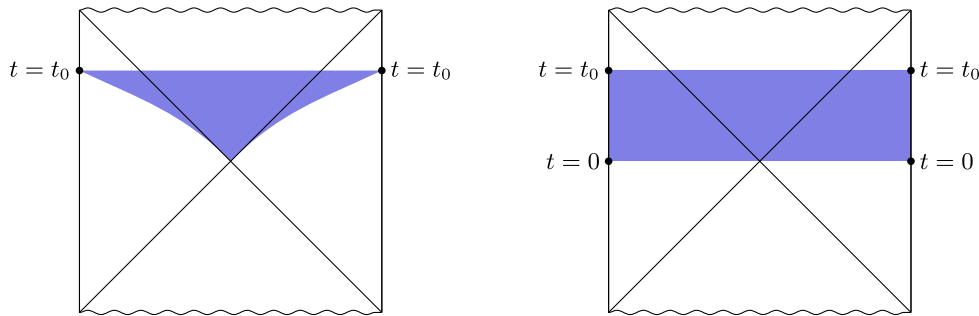


FIG. 5. Left: bulk region swept out by geodesics contributing to F_{bulk} [defined in (25)]. Right: union of all the bulk regions on the left for $0 \leq t \leq t_0$ contributing to the computational complexity $C_{\text{FS}}(t_0)$.

progress on understanding of the holographic complexity should be achievable along the lines of [14] upon the use of the holographic dictionary.

In the present paper we have recognized that the Fubini-Study cost (8) introduced in this context in [25] necessarily acquires a dual gravitational interpretation if one views boundary time evolution in the presence of sources as a quantum circuit. However, typically the gravitational counterpart is a complicated quantity as it depends on two point functions of local operators in nonequilibrium states. This led us to the setting of two-dimensional holographic CFTs in which ultimately due to the underlying Virasoro algebra we were able to construct the gravity dual to the Fubini-Study cost explicitly in terms of geodesic lengths between spacelike separated boundary points; see Fig. 2. The bulk representation of the Fubini-Study cost (26) is valid for empty AdS, conical defects and the BTZ black hole geometries. We used the latter realization to show that the Fubini-Study complexity shows the expected linear growth for the time-evolved TFD state. Finally, we demonstrated that in the presence of bulk matter fields such as shock waves the bulk quantity we introduce with (26) is no longer dual to the Fubini-Study cost. This is expected, since the geometry contains backreacting matter, and our novel gravitational quantity represents the Fubini-Study cost only in the universal sector of AdS₃ holography given by pure gravity with negative cosmological constant. Nevertheless, (26) considered more generally is interesting in these geometries since—in contrast to the boundary Fubini-study cost—the bulk quantity (26) shows the switchback effect.

There are important aspects in which the geometric object on the gravity side we constructed differs from all previous holographic complexity proposals. For clarity of presentation, let us discuss them one by one.

As described in Sec. IV, we find a linearly increasing complexity (or decreasing close to the recurrence time). However, the way the linear increase arises from the bulk perspective is different in our case than in previously proposed holographic complexity measures. In the latter case, the holographic dual to computational complexity lies within a bulk region that is spacelike to the boundary time

slice in which the target state is defined. The linear increase in this case is essentially due to the increasing size of the wormhole interior. In our work, we are integrating the quantity F_{bulk} from (25), which in this case is constant, over time. Therefore its bulk dual contains geodesics which probe the bulk region lying between the two time slices where the reference and target states are defined; see Fig. 5. Another difference is that we find a computational complexity which is UV finite.¹⁷ This is related to the fact that our reference states are energy eigenstates or a TFD state at $t = 0$ instead of a spatially unentangled state proposed as a reference state for the earlier complexity proposals in [9]. Indeed, the analyses in [19,25] showed explicitly that starting with spatially disentangled state one can mimic the leading divergence of holographic complexity proposals in the setting of free quantum fields. Therefore, our bulk dual to computational complexity realizes the features expected from complexity calculations in finite qubit systems in a somewhat different way than the conjectured holographic complexity proposals. In contrast to them, however, we have derived the relation between the boundary complexity and its bulk representation from first principles.

Furthermore, our gravity expression—while somewhat similar in spirit—does not fit in the set of holographic complexity proposals put forward in [11,12] under the slogan of “complexity = anything.” In the proposals of [11,12], holographic complexity measures are constructed by integrating functionals of the bulk metric on codimension-one or codimension-zero hypersurfaces in the bulk. These hypersurfaces are obtained by extremizing functionals of the induced metric and extrinsic curvature on either the hypersurface itself in case it is codimension-one or else on the hypersurface boundaries. Moreover, the hypersurfaces are restricted to asymptote to $t = t_0$ on the left and right asymptotic boundary of a wormhole geometry in the bulk. As mentioned above, this restriction does not hold true for the holographic complexity measure proposed in our present

¹⁷Another UV finite complexity proposal generalizing CA has been studied in [93].

work, which is defined through geodesics ending at $0 \leq t \leq t_0$ on the AdS boundary. The geometric quantity F_{bulk} dual to the Fubini-Study cost function, on the other hand, is naturally associated to a codimension-zero bulk region swept out by all geodesics anchored at $t = t_0$ (see Fig. 5) and thus constructed similarly to the complexity proposals of [12].¹⁸

In hindsight [94], another approach pursuing sources in the context of state or operator preparation in quantum field theory has been the path integral optimization [78,95–98]. These works, motivated by the multiscale renormalization ansatz (MERA) [99,100], its continuous generalization (cMERA) [101,102] and the quest for understanding its origins in geometric terms, pursued redundancies in Euclidean path integrals representing the same state preparation as an origin of an optimization procedure. There are two main differences between these results and our studies. The first one has to do with the fact that in our work we have a full control and understanding over our cost function, whereas in the one adopted in the path-integral optimization approach for Lorentzian circuits become

problematic [94]. The second one has to do the prominent role the UV cutoff plays in the optimization procedure in the case of the path-integral optimization [94,103] with our work using a UV-finite cost function. In particular, the latter has led to a new perspective on the path-integral optimization [104–107], which crucially involves coarse-graining CFT states [108,109]. In contrast, our work is entirely phrased in the language of a local operators in CFT.

The complexity measure studied in this paper does not show the saturation behavior expected in finite qubit systems. From the bulk perspective, this is not particularly surprising since the bulk dual F_{bulk} to the Fubini-Study distance we constructed is a purely classical quantity and does not take into account quantum gravity effects which were argued to lead to the saturation [81] as recently shown in two-dimensional models of quantum gravity in [28,84,110]. As it turns out, by a small modification of F_{bulk} it is also possible to obtain a total cost which saturates at an intermediate timescale. Summing only over geodesics in the BTZ geometry with winding numbers $w \leq w_{\text{max}}$ leads to an expression,

$$\tilde{F}_{\text{bulk}}(t) = \frac{2c\pi^2 \sinh\left(\frac{4\pi^2 w_{\text{max}}}{\beta}\right) \left(2 + \cosh\left(\frac{4\pi^2 w_{\text{max}}}{\beta}\right)^2 + 3 \cosh\left(\frac{4\pi^2 w_{\text{max}}}{\beta}\right) \cosh\left(\frac{4\pi t}{\beta}\right)\right)}{3\beta^3 \left(\cosh\left(\frac{4\pi^2 w_{\text{max}}}{\beta}\right) + \cosh\left(\frac{4\pi t}{\beta}\right)\right)^3}, \quad (54)$$

which is to very good approximation constant in t for $t < \pi w_{\text{max}}$ followed by a falloff exponential in t for $t > \pi w_{\text{max}}$. Integrating this in t then leads to a time-dependence as expected from Fig. 3, i.e. a linear increase followed by a plateau. The CFT interpretation of this procedure is unclear,¹⁹ as but we bring it up nevertheless as a possibly interesting model of late time holographic complexity dynamics.

Finally, we want to emphasize that the results of Sec. III relate the Fubini-Study distance to the entanglement entropy in two-dimensional holographic conformal field theories. As the expression (26) for the Fubini-Study distance involves the lengths of geodesics, which are dual to entanglement

entropies [36–39], the Fubini-Study distance is determined entirely in terms of the entanglement structure of the boundary state. Note that for states dual to conical defects and black holes, this relation naturally involves geodesics with nonzero winding number which are dual to generalized notions of entanglement entropy that account for entanglement between different fields as well as between spatial degrees of freedom, also known as entwinement [111–114]. Interestingly, these relations provide some tentative support for the idea that the modified cost function $\tilde{F}_{\text{bulk}}(t)$ defined by restricting the winding number to be smaller than some maximum can probe bulk quantum corrections as such restrictions on the maximum winding number were observed

¹⁸To see this explicitly, note that in coordinates where the BTZ metric is given by (50) and the corresponding coordinates (p, q) for the Penrose diagram defined by $U = \text{sign}(r - r_H) \sqrt{\frac{r - r_H}{r + r_H}} e^{-tr_H/L^2} = \tan(\frac{p-a}{2})$, $V = \sqrt{\frac{r - r_H}{r + r_H}} e^{tr_H/L^2} = \tan(\frac{p+a}{2})$, the codimension-one surfaces bounding the codimension-zero hypersurface shown on the left hand side of Fig. 5 are given by $t = t_0 = \text{const.}$ and $q = \arctan(\sinh t_0) = \text{const.}$ As in [12], the shape of these bounding surfaces can be obtained by extremizing a functional $G[\gamma, K]$ of the induced metric γ and extrinsic curvature K , $\delta_X \int \sqrt{\gamma} G[\gamma, K] = 0$ where X parametrizes the location of the hypersurface. For instance, for the upper bounding surface $q = q_0$ in Fig. 5, this functional can be chosen as $G[\gamma, K] = 4 + R(\gamma)^2$ where $R(\gamma)$ is the Ricci scalar associated to γ . To obtain F_{bulk} one would then need to integrate another functional of the bulk metric inside the codimension-zero hypersurface in between the two bounding surfaces.

But even though this construction works the same way as in [12], F_{bulk} is not a holographic complexity measure in the sense of [12] due to it being constant in time instead of growing linearly at late times.

¹⁹The modified cost function \tilde{F}_{bulk} does not correspond to the Fubini-Study distance which for any quantum system in a thermal state evolving with a constant Hamiltonian is constant as well and thus always leads to a linearly increasing total cost.

in [114] and attributed to finite central charge effects which disappear in the limit where the gravity theory becomes classical.

VII. OUTLOOK

The construction of the bulk dual to quantum circuits allows us to derive holographic duals to CFT cost functionals and vice versa from first principles. A natural next step is to expand the dictionary between CFT cost functionals and bulk quantities beyond the instance we identified and solved in the present work. One natural direction along these lines can build on [48] to generalize our approach to the global part of the conformal group in an arbitrary number of dimensions. Another important direction is to include additional sources on the CFT size beyond the metric, which couples to the energy-momentum tensor. Including primary operators into the picture is particularly important, as it will allow for a better understanding of the switchback effect using an entirely controllable holographic cost setup. Also, this will allow to leave the kinematic confines of the conformal group and study cost and complexity relevant to strongly coupled theories, rather than shared by all CFTs.

By construction, the gravity dual to the circuit encodes features of the auxiliary complexity geometry. We have shown how the complexity geometry metric is encoded holographically. It would be interesting to understand if other characteristics of the circuit geometry, for instance the sectional curvature considered in the context of circuits underlying our work in [20,21] and also of broader interest for complexity in quantum-many body systems [115–118], acquire a natural gravitational interpretation.

It would also be interesting to extend our setup to the lower-dimensional duality between Jackiw–Teitelboim (JT) gravity and random matrix theory. An interesting feature of this duality is that the partition function of JT gravity cannot be written as a trace over a Hilbert space of $e^{-\beta H}$ due to it being dual to an average over random matrices [119,120]. Therefore, the expression on the right-hand side of (34) whose bulk dual we found in AdS₃ is not equal to the Fubini-Study distance in the TFD state as it does not have the interpretation of a connected two-point function of the Hamiltonian in the TFD state. Rather, to determine the averaged Fubini-Study distance one has to compute

$$\overline{\langle H^2 \rangle_\beta} - \langle H \rangle_\beta^2 = \frac{\partial_\beta^2 Z(\beta)}{Z(\beta)} - \left(\frac{\partial_\beta Z(\beta)}{Z(\beta)} \right)^2, \quad (55)$$

i.e. first compute the Fubini-Study distance for a single member of the random matrix ensemble and then average. Finding a JT gravity dual to this averaged Fubini-Study distance would allow for studying quantum corrections at late times. Such corrections were already found to lead to a

plateau in the holographic complexity measures in JT gravity studied in [28,84,110]. Ensemble averages of CFTs in two and higher dimensions have recently attracted considerable attention in relation to new Euclidean worm-hole contributions to the gravitational path integral (see e.g. [121–124]). Therefore, generalizing our setup to JT gravity will likely provide further clues if and how holographic complexity measures in higher dimensions such as the one studied here saturate at late times.

We also note that computational complexity has found applications in diagnosing quantum chaos through differing saturation times for chaotic and integrable systems [125,126]. As holographic CFTs show signs of quantum chaos as well, it would be interesting to generalize our methods to probe these features. Since the chaotic features are encoded in the part of the spectrum that is not fixed by symmetry considerations such as conformal and modular transformations [127], this will require generalizing to quantum circuits transforming between different Verma modules.

Furthermore, it will be interesting to consider generalizations of our results may to higher dimensions. Quantum circuits built out of global conformal transformations as well as the Fubini-Study cost function were studied in higher dimensions in [48]. A starting point for looking at higher dimensions is an alternative proposal for a bulk dual of the Fubini-Study cost of 2D CFTs in terms of timelike geodesics in a conical defect geometry, as was put forward in the more restricted setup where only global conformal transformations act on the reference state [48]. It will therefore be interesting to derive the bulk dual of the circuit considered in [48] using similar techniques as in Sec. II. An important challenge to overcome in this regard is that in higher dimensions the dual bulk spacetime can in general be reconstructed with the Fefferman-Graham expansion only in the asymptotic region near the boundary. However, other parts of our construction, such as expressing the two-point function of the Hamiltonian in terms of a UV finite expression involving geodesic lengths, are likely to also apply in higher dimensions.²⁰

Finally, the Virasoro algebra that constitutes a crucial ingredient in our construction also emerges in a variety of discrete systems such as spin chains and their tensor network description [128–135]. It will be interesting to connect with complexity studies in these quantum-many body settings, in light of recent advancements [117,136,137] on computational complexity in discrete systems in the framework of [14] that we also employed here.

²⁰The UV finiteness is a result of the fact that the UV regulator drops out after taking derivatives of geodesic lengths with respect to the location of their end points. This property continues to hold in higher dimensions.

ACKNOWLEDGMENTS

We would like to thank Mario Flory for his involvement in the early stages of this project. Moreover, we thank Paweł Caputa, Shira Chapman, Bartek Czech, Jan de Boer, Juan Hernandez, Mikhael Khramtsov, Rob Myers, Tadashi Takayanagi, and Qi-Feng Wu for useful discussions and correspondence. The work of A.-L. W. is supported by DFG, Grant No. ER 301/8-1—ME 5047/2-1. The work of J. E. and M. G. was supported by Germany’s Excellence Strategy through the Würzburg-Dresden Cluster of Excellence on Complexity and Topology in Quantum Matter ct.qmat (EXC 2147, projectid 390858490), as well as through the German-Israeli Project Cooperation (DIP) grant “Holography and the Swampland” This research has also been supported by FWO-Vlaanderen project G012222N and by Vrije Universiteit Brussel through the Strategic Research Program High-Energy Physics. Moreover, this research was supported in part by Perimeter Institute for Theoretical Physics. Research at Perimeter Institute is supported by the Government of Canada through the Department of Innovation, Science and Economic Development and by the Province of Ontario through the Ministry of Research, Innovation and Science.

APPENDIX A: LESSONS FROM $SL(2, \mathbb{R})$ CIRCUITS

In this appendix we compare our geometrization of the Fubini-Study metric in the holographic bulk spacetime with the construction in [48] for $SL(2, \mathbb{R})$ circuits.

The authors of [48] considered circuits implementing global conformal transformations in $d \geq 2$. For a more direct comparison with our work, we discuss only CFTs in two dimensions. In this setup, the global conformal transformations form the symmetry group $SL(2, \mathbb{R})$, and diffeomorphisms may be parametrized in terms of three parameters $\gamma_R(\tau), \zeta(\tau), \zeta^*(\tau)$,

$$F(\tau, x^\pm) = -i \log \left(\frac{i e^{i(x^\pm + \gamma_R(\tau))} - \zeta(\tau)}{i + e^{i(x^\pm + \gamma_R(\tau))} \zeta^*(\tau)} \right), \quad (\text{A1})$$

where x^\pm are light cone coordinates on the cylinder. The circuit corresponding to (A1) is given by

$$U(\tau)|h\rangle \equiv e^{i\zeta(\tau)L_{-1}} e^{i\gamma(\tau)L_0} e^{i\zeta_1(\tau)L_1}|h\rangle, \quad (\text{A2})$$

where $\gamma(\tau) = \gamma_R(\tau) - i \log(1 - |\zeta|^2)$ and $\zeta_1(\tau) = \zeta^*(\tau) e^{i\gamma_R(\tau)}$. Note that the transformation (A1) is a symmetry of the CFT in the vacuum state. Therefore, an appropriate reference state for such circuits is $|h\rangle$ with $h > 0$. The Fubini-Study distance for (A1) is given by

$$ds_{\text{FS}}^2 = 2h \frac{d\zeta d\zeta^*}{(1 - |\zeta|^2)^2}. \quad (\text{A3})$$

In the gravity theory, the reference state $|h\rangle$ in the CFT circuit corresponds to a conical defect geometry,

$$ds_{\text{AdS}}^2 = d\rho^2 - \cosh \rho^2 dt^2 + \sinh^2(\rho) d\phi^2, \quad (\text{A4})$$

where ϕ is $\frac{2\pi}{n}$ -periodic and $n \in \mathbb{N}$. The geometry can be interpreted as empty AdS with a particle of mass m located at the center $\rho = 0, t = 0, \phi = 0$. As it moves along a timelike trajectory, the massive particle cuts out a wedge related to its mass, $m = -1/8Gn^2$ [59].

The authors of [48] then observed that the symplectic geometry associated to the circuit generated by the transformations (A1) is equivalent to that of timelike geodesics in AdS. This equivalence indicates that geometric features of the phase space such as the Fubini-Study distance (A3) may be written in terms of timelike geodesics. The timelike geodesics corresponding to the circuit arising from (A1) may be obtained by considering the empty AdS geodesic $(\rho(t), t, \phi(t)) = (0, t, 0)$ and boosting it by (A1), which yields a sequence of geodesics in a single geometry. It is convenient to rewrite the geodesics in terms of embedding-space coordinates,

$$\begin{aligned} T_1 &= \cosh(\rho(t)) \cos(t), \\ T_2 &= \cosh(\rho(t)) \sin(t), \\ X_1 &= \sinh(\rho(t)) \cos(\phi(t)), \\ X_2 &= \sinh(\rho(t)) \sin(\phi(t)), \end{aligned} \quad (\text{A5})$$

with metric $ds^2 = -dT_1^2 - dT_2^2 + dX_1^2 + dX_2^2$. If we apply only a left-moving transformation (A1), the geodesics read

$$\begin{aligned} \phi(t) &= \arctan \left(i + \frac{2i\zeta^*}{e^{2it}\zeta - \zeta^*} \right), \\ \rho(t) &= \text{arcsech} \left(\sqrt{1 - |\zeta|^2} \right). \end{aligned} \quad (\text{A6})$$

By X^μ we now denote the vector $X^\mu = \{X_1, X_2\}$. The Fubini-Study distance is then given in terms of the minimal and maximal distance between two such geodesics [48],

$$ds_{\text{FS}}^2 = \frac{h}{2} (\delta X_{\text{perp.min}}^2 + \delta X_{\text{perp.max}}^2). \quad (\text{A7})$$

Let us now highlight some important differences to our construction of a dual to the Fubini-Study metric. First of all, the result (A7) relies on the identification of the configuration space $(\zeta, \zeta^*, \gamma_R)$ associated to the circuit and the phase space of timelike geodesics in AdS. It is therefore not straightforward to generalize (A7) to

geometries other than the conical defect and to transformations beyond $SL(2, \mathbb{R})$. A general conformal transformation in two dimensions, which is the focus of our work, is parametrized by an infinite number of parameters and therefore can no longer be identified with the phase space of a massive particle. Furthermore, in [48], there is no dual to the circuit itself in the bulk geometry. Instead, a state in the CFT corresponds to a geodesic along its full trajectory and multiple boosted geodesics representing the states in the circuit are considered within the same geometry. On the other hand, in our construction, the state is defined on a constant time slice in the CFT and extends into the bulk to the full Wheeler-De Witt patch. The evolution of the state according to the circuit is encoded in the time evolution of the geometry. In particular, physical time has no significance in (A7) and is eliminated by the extremization procedure.

Finding a similar realization of the Fubini-Study distance in terms of timelike geodesics in our setup is not straightforward as the timelike geodesics considered in [48] differ in another important aspect from our construction: The $U(1)$ transformation $x^+ \rightarrow x^+ + \gamma_R(\tau)$ constitutes a global symmetry and leaves the timelike geodesic invariant. The $U(1)$ transformation acts on each constant time slice by shifting it by a value $\gamma_R(\tau)$ that is constant with respect to the physical time t . In our construction, the identification $\tau = t$ implies that a similar $U(1)$ transformation $x^+ \rightarrow x^+ + \alpha(t)$ acts differently on each constant time slices as the shift $\alpha(t)$ now depends on physical time. Timelike geodesics in this case start exhibiting $\alpha(t)$ -dependence. Since we know that $\alpha(t)$ does not enter the Fubini-Study distance, it is therefore natural to consider a geometric object that we already know to share this property instead. This is the length of spacelike geodesics on a constant time slice, which is the main ingredient of our cost measure, as discussed in Sec. III.

APPENDIX B: THE SWITCHBACK EFFECT IN DELOCALIZED AND BLACK STRING SHOCK WAVES

In order to determine how universal the switchback effects found in Sec. V are, in this appendix we study the geometric expression F_{bulk} from (25) in further shock wave geometries than the ones considered in Sec. V. We consider shock waves in a black string geometry, i.e. a black hole with noncompact horizon, as well as delocalized shock waves where the matter is concentrated uniformly in the angular direction. We find that in both cases the switchback effect is reproduced qualitatively in the sense that F_{bulk} increases with increasing t_W before saturating to the variance of the Hamiltonian in the TFD state. From a quantitative perspective the match to the expectations from the infection models from [7,81] is not quite as good as for

the localized shock waves in the BTZ black hole geometry considered in Sec. V. Note, however, that the infection models are very simplified versions of the full gravity setup which in particular are based on the assumption of an initially spatially localized perturbation spreading throughout a finite size system. With this caveat in mind, it is not surprising that our result deviate somewhat from the results of the infection models when these assumptions are violated.

1. Delocalized shock waves

We will start with simple shock wave geometries where the shock wave is delocalized in the space direction (but still localized at the horizon) used for instance in [7]. In this case, the solution of Einstein's equation is given by (46) with a displacement function $h(\phi) = \alpha$ that is constant along the spatial direction. The geodesic length from the left boundary to the point $(u = 0, v = v_s + \alpha, \phi = \phi_s)$ on the left side of the shock wave is given by

$$\ell_1 = \log \left[\frac{e^{r_H t_1} (v_s + \alpha) + \cosh(r_H (\phi_1 - \phi_s))}{\sqrt{\epsilon_{\text{UV}}}} \right], \quad (\text{B1})$$

and the length from the point $(u = 0, v = v_s, \phi = \phi_s)$ on the right side of the shock wave to the right boundary by

$$\ell_2 = \log \left[\frac{-e^{-r_H t_2} v_s + \cosh(r_H (\phi_2 - \phi_s))}{\sqrt{\epsilon_{\text{UV}}}} \right]. \quad (\text{B2})$$

The total geodesic length is given by

$$\ell = \log \left[\frac{1}{\epsilon_{\text{UV}}} \left(\sqrt{\frac{1}{2} \cosh(r_H (\phi_1 - \phi_2)) + \frac{1}{2} \cosh(r_H (t_1 + t_2))} + \frac{\alpha}{2} e^{r_H (t_1 - t_2)/2} \right)^2 \right]. \quad (\text{B3})$$

Taking into account only these geodesics between different asymptotic boundaries we find again a time delay in t_W before the Fubini-Study distance saturates (see Fig. 6), and thus the total Fubini-Study cost (35) increases linearly with a time delay. These features qualitatively reproduce the switchback effect. However, in this case F_{bulk} is negative in some parameter regimes which is not sensible for a cost function for computational complexity, and hence F_{bulk} can no longer be interpreted as the gravity analog of the number of infected qubits in the model of [7,81]. As the delocalized shock waves are more akin to a delocalized perturbation W acting on the whole system instead of the localized perturbation acting on a single qubit considered in [7,81], this match in qualitative but not quantitative terms is not too

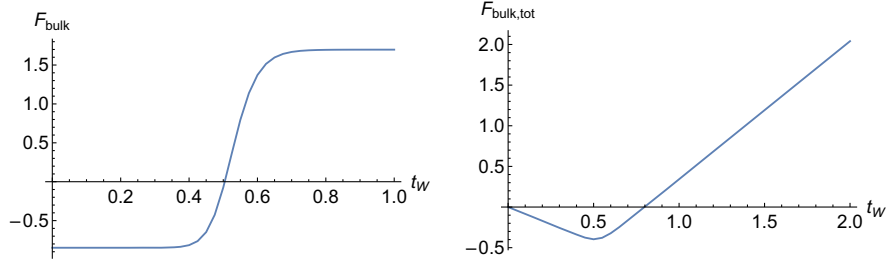


FIG. 6. Left: F_{bulk} plotted over t_W and right: the corresponding total cost $F_{\text{bulk,tot}}$ (the t_W integral of F_{bulk}) in a BTZ geometry perturbed by a single delocalized shock wave with strength α from (45) and $t_* = 0.5$, $\beta = 1/4$.

surprising. However F_{bulk} is also bounded from below by $-\frac{1}{2}$ times the thermal two-point function $\langle H^2 \rangle_\beta - \langle H \rangle_\beta^2$. By also including geodesics stretching between points on the same asymptotic boundaries which are not modified by the introduction of the shock wave, F_{bulk} acquires an additional positive contribution $\langle H^2 \rangle_\beta - \langle H \rangle_\beta^2$ that ensures positivity of the total result.

2. Localized shock waves with non-compact horizon

Another class of shock wave geometries are those with non-compact horizon and localized matter concentrations studied in [92]. In this case, a localized shock wave corresponds to a metric (46) with displacement,

$$v \rightarrow v + h(\phi) \quad \text{with} \quad h(\phi) = \alpha e^{-|\phi - \hat{\phi}| r_H}, \quad (\text{B4})$$

where $\hat{\phi}$ is a constant parameter and $-\infty < \phi < \infty$. This is obtained by solving Einstein's equations with an energy concentration localized at the $u = 0$ horizon and at $\phi = \hat{\phi}$ [90],

$$T_{uu} = \frac{\alpha}{2\pi G_N} \delta(u) \delta(\phi - \hat{\phi}) \quad \text{and} \quad T_{\mu\nu} = 0, \quad (\mu, \nu) \neq (u, u). \quad (\text{B5})$$

The geodesic lengths are given by

$$\begin{aligned} \ell_1 &= \log \left[\frac{e^{r_H t_1} (v_s + h(\phi_s)) + \cosh(r_H(\phi_1 - \phi_s))}{\sqrt{\epsilon_{UV}}} \right], \\ \ell_2 &= \log \left[\frac{-e^{-r_H t_2} v_s + \cosh(r_H(\phi_2 - \phi_s))}{\sqrt{\epsilon_{UV}}} \right], \end{aligned} \quad (\text{B6})$$

and

$$\begin{aligned} \ell &= \log[\cosh(r_H(\bar{t} \pm \Delta\phi))(\cosh(r_H(\bar{t} \mp \Delta\phi)) \\ &\quad + \alpha e^{r_H(\pm \hat{\phi} \mp \bar{\phi} + \Delta t)}), \end{aligned} \quad (\text{B7})$$

with $\pm = \text{sgn}(\bar{\phi} - \hat{\phi} - \frac{1}{2r_H} \log(\frac{\cosh(r_H(\bar{t} - \Delta\phi))}{\cosh(r_H(\bar{t} + \Delta\phi))}))$ where $\bar{\phi} = (\phi_1 + \phi_2)/2$, $\Delta\phi = (\phi_1 - \phi_2)/2$, $\bar{t} = (t_1 + t_2)/2$, $\Delta t = (t_1 - t_2)/2$. The results for F_{bulk} from (26) are qualitatively similar to the case of a localized shock wave with compact horizon studied in Sec. V. Again, we find an increase of F_{FS} followed by a saturation if t_W and with it the shock wave strength α is varied while $t = 0$ is kept constant. Unlike for the compact horizon case, however, here we find that F_{bulk} does not asymptote to zero for $t_W \rightarrow 0$. In the infection model of [7,81], this may be interpreted as a perturbation W which is so large that already at $t_W = 0$ a sizeable fraction of the system is infected.

-
- [1] J. M. Maldacena, The large N limit of superconformal field theories and supergravity, *Adv. Theor. Math. Phys.* **2**, 231 (1998).
 [2] S. S. Gubser, I. R. Klebanov, and A. M. Polyakov, Gauge theory correlators from noncritical string theory, *Phys. Lett. B* **428**, 105 (1998).
 [3] E. Witten, Anti-de Sitter space and holography, *Adv. Theor. Math. Phys.* **2**, 253 (1998).

- [4] L. Susskind, Computational complexity and black hole horizons, *Fortschr. Phys.* **64**, 24 (2014).
 [5] S. Aaronson, The complexity of quantum states and transformations: From quantum money to black holes, [arXiv:1607.05256](https://arxiv.org/abs/1607.05256).
 [6] S. Chapman and G. Policastro, Quantum computational complexity from quantum information to black holes and back, *Eur. Phys. J. C* **82**, 128 (2022).

- [7] D. Stanford and L. Susskind, Complexity and shock wave geometries, *Phys. Rev. D* **90**, 126007 (2014).
- [8] A. R. Brown, D. A. Roberts, L. Susskind, B. Swingle, and Y. Zhao, Holographic Complexity Equals Bulk Action?, *Phys. Rev. Lett.* **116**, 191301 (2016).
- [9] A. R. Brown, D. A. Roberts, L. Susskind, B. Swingle, and Y. Zhao, Complexity, action, and black holes, *Phys. Rev. D* **93**, 086006 (2016).
- [10] J. Couch, W. Fischler, and P. H. Nguyen, Noether charge, black hole volume, and complexity, *J. High Energy Phys.* **03** (2017) 119.
- [11] A. Belin, R. C. Myers, S.-M. Ruan, G. Sárosi, and A. J. Speranza, Does Complexity Equal Anything?, *Phys. Rev. Lett.* **128**, 081602 (2022).
- [12] A. Belin, R. C. Myers, S.-M. Ruan, G. Sárosi, and A. J. Speranza, Complexity equals anything II, *J. High Energy Phys.* **01** (2023) 154.
- [13] J. M. Maldacena, Eternal black holes in anti-de Sitter, *J. High Energy Phys.* **04** (2003) 021.
- [14] M. A. Nielsen, A geometric approach to quantum circuit lower bounds, *Quantum Inf. Comput.* **6**, 213 (2006).
- [15] K. Skenderis and B. C. van Rees, Real-Time Gauge/Gravity Duality, *Phys. Rev. Lett.* **101**, 081601 (2008).
- [16] K. Skenderis and B. C. van Rees, Real-time gauge/gravity duality: Prescription, renormalization and examples, *J. High Energy Phys.* **05** (2009) 085.
- [17] J. Erdmenger, M. Flory, M. Gerbershagen, M. P. Heller, and A.-L. Weigel, Exact gravity duals for simple quantum circuits, *SciPost Phys.* **13**, 061 (2022).
- [18] I. Bengtsson and K. Życzkowski, *Geometry of Quantum States: An Introduction to Quantum Entanglement* (Cambridge University Press, Cambridge, England, 2017), 2nd ed.
- [19] R. Jefferson and R. C. Myers, Circuit complexity in quantum field theory, *J. High Energy Phys.* **10** (2017) 107.
- [20] M. Flory and M. P. Heller, Conformal field theory complexity from Euler-Arnold equations, *J. High Energy Phys.* **12** (2020) 091.
- [21] M. Flory and M. P. Heller, Geometry of complexity in conformal field theory, *Phys. Rev. Res.* **2**, 043438 (2020).
- [22] L. Hackl and R. C. Myers, Circuit complexity for free fermions, *J. High Energy Phys.* **07** (2018) 139.
- [23] S. Chapman, J. Eisert, L. Hackl, M. P. Heller, R. Jefferson, H. Marrochio, and R. C. Myers, Complexity and entanglement for thermofield double states, *SciPost Phys.* **6**, 034 (2019).
- [24] P. Bueno, J. M. Magan, and C. S. Shahbazi, Complexity measures in QFT and constrained geometric actions, *J. High Energy Phys.* **09** (2021) 200.
- [25] S. Chapman, M. P. Heller, H. Marrochio, and F. Pastawski, Toward a Definition of Complexity for Quantum Field Theory States, *Phys. Rev. Lett.* **120**, 121602 (2018).
- [26] R. Khan, C. Krishnan, and S. Sharma, Circuit complexity in fermionic field theory, *Phys. Rev. D* **98**, 126001 (2018).
- [27] P. Caputa and J. M. Magan, Quantum Computation as Gravity, *Phys. Rev. Lett.* **122**, 231302 (2019).
- [28] M. Alishahiha, S. Banerjee, and J. Kames-King, Complexity via replica trick, *J. High Energy Phys.* **08** (2022) 181.
- [29] P. M. Chesler and D. Teaney, Dynamical Hawking radiation and holographic thermalization, [arXiv:1112.6196](https://arxiv.org/abs/1112.6196).
- [30] P. M. Chesler and D. Teaney, Dilaton emission and absorption from far-from-equilibrium non-Abelian plasma, [arXiv:1211.0343](https://arxiv.org/abs/1211.0343).
- [31] V. Keranen and P. Kleinert, Non-equilibrium scalar two point functions in AdS/CFT, *J. High Energy Phys.* **04** (2015) 119.
- [32] H. Liu and J. Sonner, Holographic systems far from equilibrium: A review, *Rep. Prog. Phys.* **83**, 016001 (2019).
- [33] M. Bianchi, D. Z. Freedman, and K. Skenderis, Holographic renormalization, *Nucl. Phys.* **B631**, 159 (2002).
- [34] J. M. Maldacena, Wilson Loops in Large N Field Theories, *Phys. Rev. Lett.* **80**, 4859 (1998).
- [35] S.-J. Rey and J.-T. Yee, Macroscopic strings as heavy quarks in large N gauge theory and anti-de Sitter supergravity, *Eur. Phys. J. C* **22**, 379 (2001).
- [36] S. Ryu and T. Takayanagi, Holographic Derivation of Entanglement Entropy from AdS/CFT, *Phys. Rev. Lett.* **96**, 181602 (2006).
- [37] V. E. Hubeny, M. Rangamani, and T. Takayanagi, A covariant holographic entanglement entropy proposal, *J. High Energy Phys.* **07** (2007) 062.
- [38] A. Lewkowycz and J. Maldacena, Generalized gravitational entropy, *J. High Energy Phys.* **08** (2013) 090.
- [39] X. Dong, A. Lewkowycz, and M. Rangamani, Deriving covariant holographic entanglement, *J. High Energy Phys.* **11** (2016) 028.
- [40] X. Dong, The gravity dual of Renyi entropy, *Nat. Commun.* **7**, 12472 (2016).
- [41] J. M. Magán, Black holes, complexity and quantum chaos, *J. High Energy Phys.* **09** (2018) 043.
- [42] I. Akal, Reflections on Virasoro circuit complexity and Berry phase, *Phys. Rev. D* **105**, 025012 (2022).
- [43] J. Erdmenger, M. Gerbershagen, and A.-L. Weigel, Complexity measures from geometric actions on Virasoro and Kac-Moody orbits, *J. High Energy Phys.* **11** (2020) 003.
- [44] R. d. M. Koch, M. Kim, and H. J. R. Van Zyl, Complexity from spinning primaries, *J. High Energy Phys.* **12** (2021) 030.
- [45] A. Belin, A. Lewkowycz, and G. Sárosi, Complexity and the bulk volume, a New York Time story, *J. High Energy Phys.* **03** (2019) 044.
- [46] M. Flory and N. Miekley, Complexity change under conformal transformations in AdS₃/CFT₂, *J. High Energy Phys.* **05** (2019) 003.
- [47] M. Flory, WdW-patches in AdS₃ and complexity change under conformal transformations II, *J. High Energy Phys.* **05** (2019) 086.
- [48] N. Chagnet, S. Chapman, J. de Boer, and C. Zukowski, Complexity for Conformal Field Theories in General Dimensions, *Phys. Rev. Lett.* **128**, 051601 (2022).
- [49] P. Caputa and D. Ge, Entanglement and geometry from subalgebras of the Virasoro, *J. High Energy Phys.* **06** (2023) 159.

- [50] M. Miyaji, T. Numasawa, N. Shiba, T. Takayanagi, and K. Watanabe, Distance between Quantum States and Gauge-Gravity Duality, *Phys. Rev. Lett.* **115**, 261602 (2015).
- [51] N. Lashkari and M. Van Raamsdonk, Canonical energy is quantum Fisher information, *J. High Energy Phys.* **04** (2016) 153.
- [52] D. Bak, Information metric and Euclidean Janus correspondence, *Phys. Lett. B* **756**, 200 (2016).
- [53] A. Trivella, Holographic computations of the quantum information metric, *Classical Quantum Gravity* **34**, 105003 (2017).
- [54] M. Miyaji, Butterflies from information metric, *J. High Energy Phys.* **09** (2016) 002.
- [55] S. Banerjee, J. Erdmenger, and D. Sarkar, Connecting Fisher information to bulk entanglement in holography, *J. High Energy Phys.* **08** (2018) 001.
- [56] M. Flory, A complexity/fidelity susceptibility g -theorem for AdS₃/BCFT₂, *J. High Energy Phys.* **06** (2017) 131.
- [57] D. Bak and A. Trivella, Quantum information metric on $\mathbb{R} \times S^{d-1}$, *J. High Energy Phys.* **09** (2017) 086.
- [58] X.-B. Xu, S.-Q. Lan, G.-Q. Li, and J.-X. Mo, A simple analysis of the mixed-state information metric in AdS₃/CFT₂, *Mod. Phys. Lett. A* **34**, 1950334 (2019).
- [59] C.-B. Chen, W.-C. Gan, F.-W. Shu, and B. Xiong, Quantum information metric of conical defect, *Phys. Rev. D* **98**, 046008 (2018).
- [60] H. Dimov, I. N. Iliev, M. Radomirov, R. C. Rashkov, and T. Vetsov, Holographic Fisher information metric in Schrödinger spacetime, *Eur. Phys. J. Plus* **136**, 1128 (2021).
- [61] A. Tsuchiya and K. Yamashiro, A geometrical representation of the quantum information metric in the gauge/gravity correspondence, *Phys. Lett. B* **824**, 136830 (2022).
- [62] L. Susskind and Y. Zhao, Switchbacks and the bridge to nowhere, [arXiv:1408.2823](https://arxiv.org/abs/1408.2823).
- [63] C. Fefferman and C. R. Graham, Conformal invariants, in *Élie Cartan et les mathématiques d'aujourd'hui—Lyon, 25–29 juin 1984*, no. S131 in Astérisque (Société mathématique de France, 1985).
- [64] S. de Haro, S. N. Solodukhin, and K. Skenderis, Holographic reconstruction of space-time and renormalization in the AdS/CFT correspondence, *Commun. Math. Phys.* **217**, 595 (2001).
- [65] L. A. Santaló, *Integral Geometry and Geometric Probability* (Addison-Wesley, Reading, MA, 1976).
- [66] B. Czech, L. Lamprou, S. McCandlish, and J. Sully, Integral geometry and holography, *J. High Energy Phys.* **10** (2015) 175.
- [67] B. Czech and L. Lamprou, Holographic definition of points and distances, *Phys. Rev. D* **90**, 106005 (2014).
- [68] B. Czech, L. Lamprou, S. McCandlish, and J. Sully, Tensor networks from kinematic space, *J. High Energy Phys.* **07** (2016) 100.
- [69] J. de Boer, M. P. Heller, R. C. Myers, and Y. Neiman, Holographic de Sitter Geometry from Entanglement in Conformal Field Theory, *Phys. Rev. Lett.* **116**, 061602 (2016).
- [70] B. Czech, L. Lamprou, S. McCandlish, B. Mosk, and J. Sully, A stereoscopic look into the bulk, *J. High Energy Phys.* **07** (2016) 129.
- [71] J. de Boer, F. M. Haehl, M. P. Heller, and R. C. Myers, Entanglement, holography and causal diamonds, *J. High Energy Phys.* **08** (2016) 162.
- [72] B. Czech, L. Lamprou, S. McCandlish, and J. Sully, Modular Berry connection for entangled subregions in AdS/CFT, *Phys. Rev. Lett.* **120**, 091601 (2018).
- [73] J. C. Cresswell and A. W. Peet, Kinematic space for conical defects, *J. High Energy Phys.* **11** (2017) 155.
- [74] J.-d. Zhang and B. Chen, Kinematic space and wormholes, *J. High Energy Phys.* **01** (2017) 092.
- [75] R. Abt, J. Erdmenger, H. Hinrichsen, C. M. Melby-Thompson, R. Meyer, C. Northe, and I. A. Reyes, Topological complexity in AdS₃/CFT₂, *Fortschr. Phys.* **66**, 1800034 (2018).
- [76] R. Abt, J. Erdmenger, M. Gerbershagen, C. M. Melby-Thompson, and C. Northe, Holographic subregion complexity from kinematic space, *J. High Energy Phys.* **01** (2019) 012.
- [77] B. Czech, Y. D. Olivas, and Z.-z. Wang, Holographic integral geometry with time dependence, *J. High Energy Phys.* **12** (2020) 063.
- [78] B. Czech, Einstein Equations from Varying Complexity, *Phys. Rev. Lett.* **120**, 031601 (2018).
- [79] B. Chen, B. Czech, and Z.-z. Wang, Query complexity and cutoff dependence of the CFT₂ ground state, *Phys. Rev. D* **103**, 026015 (2021).
- [80] A. R. Brown and L. Susskind, Second law of quantum complexity, *Phys. Rev. D* **97**, 086015 (2018).
- [81] L. Susskind, Three lectures on complexity and black holes, in *Three Lectures on Complexity and Black Holes* (Springer, Cham, 2020).
- [82] J. Haferkamp, P. Faist, N. B. T. Kothakonda, J. Eisert, and N. Y. Halpern, Linear growth of quantum circuit complexity, *Nat. Phys.* **18**, 528 (2022).
- [83] M. Oszmaniec, M. Horodecki, and N. Hunter-Jones, Saturation and recurrence of quantum complexity in random quantum circuits, [arXiv:2205.09734](https://arxiv.org/abs/2205.09734).
- [84] L. V. Iliesiu, M. Mezei, and G. Sárosi, The volume of the black hole interior at late times, *J. High Energy Phys.* **07** (2022) 073.
- [85] P. Gao, D. L. Jafferis, and A. C. Wall, Traversable wormholes via a double trace deformation, *J. High Energy Phys.* **12** (2017) 151.
- [86] T. Eguchi and H. Ooguri, Conformal and current algebras on general Riemann surface, *Nucl. Phys.* **B282**, 308 (1987).
- [87] V. Balasubramanian, M. Decross, A. Kar, and O. Parrikar, Quantum complexity of time evolution with chaotic Hamiltonians, *J. High Energy Phys.* **01** (2020) 134.
- [88] A. Bernamonti, F. Galli, J. Hernandez, R. C. Myers, S.-M. Ruan, and J. Simón, Aspects of the first law of complexity, *J. Phys. A* **53**, 29 (2020).
- [89] V. Balasubramanian, M. DeCross, A. Kar, Y. C. Li, and O. Parrikar, Complexity growth in integrable and chaotic models, *J. High Energy Phys.* **07** (2021) 011.
- [90] D. A. Roberts and D. Stanford, Two-Dimensional Conformal Field Theory and the Butterfly Effect, *Phys. Rev. Lett.* **115**, 131603 (2015).

- [91] S.H. Shenker and D. Stanford, Black holes and the butterfly effect, *J. High Energy Phys.* **03** (2014) 067.
- [92] D. A. Roberts, D. Stanford, and L. Susskind, Localized shocks, *J. High Energy Phys.* **03** (2015) 051.
- [93] A. Mounim and W. Mück, Reparameterization dependence is useful for holographic complexity, *J. High Energy Phys.* **07** (2021) 010.
- [94] H. A. Camargo, M. P. Heller, R. Jefferson, and J. Knaute, Path Integral Optimization as Circuit Complexity, *Phys. Rev. Lett.* **123**, 011601 (2019).
- [95] P. Caputa, N. Kundu, M. Miyaji, T. Takayanagi, and K. Watanabe, Anti-de Sitter Space from Optimization of Path Integrals in Conformal Field Theories, *Phys. Rev. Lett.* **119**, 071602 (2017).
- [96] P. Caputa, N. Kundu, M. Miyaji, T. Takayanagi, and K. Watanabe, Liouville action as path-integral complexity: From continuous tensor networks to AdS/CFT, *J. High Energy Phys.* **11** (2017) 097.
- [97] A. Bhattacharyya, P. Caputa, S. R. Das, N. Kundu, M. Miyaji, and T. Takayanagi, Path-integral complexity for perturbed CFTs, *J. High Energy Phys.* **07** (2018) 086.
- [98] T. Takayanagi, Holographic spacetimes as quantum circuits of path-integrations, *J. High Energy Phys.* **12** (2018) 048.
- [99] G. Vidal, Entanglement Renormalization, *Phys. Rev. Lett.* **99**, 220405 (2007).
- [100] G. Evenbly and G. Vidal, Tensor Network Renormalization Yields the Multiscale Entanglement Renormalization Ansatz, *Phys. Rev. Lett.* **115**, 200401 (2015).
- [101] J. Haegeman, T. J. Osborne, H. Verschelde, and F. Verstraete, Entanglement Renormalization for Quantum Fields in Real Space, *Phys. Rev. Lett.* **110**, 100402 (2013).
- [102] M. Nozaki, S. Ryu, and T. Takayanagi, Holographic geometry of entanglement renormalization in quantum field theories, *J. High Energy Phys.* **10** (2012) 193.
- [103] P. Caputa, J. Kruthoff, and O. Parrikar, Building tensor networks for holographic states, *J. High Energy Phys.* **05** (2021) 009; **09** (2022) 112(E).
- [104] J. Boruch, P. Caputa, and T. Takayanagi, Path-integral optimization from Hartle-Hawking wave function, *Phys. Rev. D* **103**, 046017 (2021).
- [105] A. R. Chandra, J. de Boer, M. Flory, M. P. Heller, S. Hörtner, and A. Rolph, Spacetime as a quantum circuit, *J. High Energy Phys.* **04** (2021) 207.
- [106] J. Boruch, P. Caputa, D. Ge, and T. Takayanagi, Holographic path-integral optimization, *J. High Energy Phys.* **07** (2021) 016.
- [107] A. R. Chandra, J. de Boer, M. Flory, M. P. Heller, S. Hörtner, and A. Rolph, Cost of holographic path integrals, *SciPost Phys.* **14**, 061 (2023).
- [108] A. B. Zamolodchikov, Expectation value of composite field T anti- T in two-dimensional quantum field theory, [arXiv:hep-th/0401146](https://arxiv.org/abs/hep-th/0401146).
- [109] L. McGough, M. Mezei, and H. Verlinde, Moving the CFT into the bulk with $T\bar{T}$, *J. High Energy Phys.* **04** (2018) 010.
- [110] M. Alishahiha and S. Banerjee, On the saturation of late-time growth of complexity in supersymmetric JT gravity, *J. High Energy Phys.* **01** (2023) 134.
- [111] V. Balasubramanian, B. D. Chowdhury, B. Czech, and J. de Boer, Entwinement and the emergence of spacetime, *J. High Energy Phys.* **01** (2015) 048.
- [112] V. Balasubramanian, A. Bernamonti, B. Craps, T. De Jonckheere, and F. Galli, Entwinement in discretely gauged theories, *J. High Energy Phys.* **12** (2016) 094.
- [113] V. Balasubramanian, B. Craps, T. De Jonckheere, and G. Sárosi, Entanglement versus entwinement in symmetric product orbifolds, *J. High Energy Phys.* **01** (2019) 190.
- [114] M. Gerbershagen, Illuminating entanglement shadows of BTZ black holes by a generalized entanglement measure, *J. High Energy Phys.* **10** (2021) 187.
- [115] R. Auzzi, S. Baiguera, G. B. De Luca, A. Legramandi, G. Nardelli, and N. Zenoni, Geometry of quantum complexity, *Phys. Rev. D* **103**, 106021 (2021).
- [116] Q.-F. Wu, Sectional curvatures distribution of complexity geometry, *J. High Energy Phys.* **08** (2022) 197.
- [117] A. R. Brown, A quantum complexity lowerbound from differential geometry, *Nat. Phys.* **19**, 401 (2023).
- [118] P. Basteiro, J. Erdmenger, P. Fries, F. Goth, I. Matthaiakakis, and R. Meyer, Quantum complexity as hydrodynamics, *Phys. Rev. D* **106**, 065016 (2022).
- [119] D. Stanford and E. Witten, Fermionic localization of the Schwarzian theory, *J. High Energy Phys.* **10** (2017) 008.
- [120] P. Saad, S. H. Shenker, and D. Stanford, JT gravity as a matrix integral, [arXiv:1903.11115](https://arxiv.org/abs/1903.11115).
- [121] J. Cotler and K. Jensen, A precision test of averaging in AdS/CFT, *J. High Energy Phys.* **11** (2022) 070.
- [122] A. Belin and J. de Boer, Random statistics of OPE coefficients and Euclidean wormholes, *Classical Quantum Gravity* **38**, 164001 (2021).
- [123] N. Afkhami-Jeddi, H. Cohn, T. Hartman, and A. Tajdini, Free partition functions and an averaged holographic duality, *J. High Energy Phys.* **01** (2021) 130.
- [124] A. Maloney and E. Witten, Averaging over Narain moduli space, *J. High Energy Phys.* **10** (2020) 187.
- [125] B. Craps, M. De Clerck, O. Evnin, P. Hacker, and M. Pavlov, Bounds on quantum evolution complexity via lattice cryptography, *SciPost Phys.* **13**, 090 (2022).
- [126] B. Craps, M. De Clerck, O. Evnin, and P. Hacker, Integrability and complexity in quantum spin chains, [arXiv:2305.00037](https://arxiv.org/abs/2305.00037).
- [127] F. M. Haehl, C. Marteau, W. Reeves, and M. Rozali, Symmetries and spectral statistics in chaotic conformal field theories, *J. High Energy Phys.* **07** (2023) 196.
- [128] W. M. Koo and H. Saleur, Representations of the Virasoro algebra from lattice models, *Nucl. Phys.* **B426**, 459 (1994).
- [129] A. Milsted and G. Vidal, Extraction of conformal data in critical quantum spin chains using the Koo-Saleur formula, *Phys. Rev. B* **96**, 245105 (2017).
- [130] Y. Zou, A. Milsted, and G. Vidal, Conformal Data and Renormalization Group Flow in Critical Quantum Spin Chains using Periodic Uniform Matrix Product States, *Phys. Rev. Lett.* **121**, 230402 (2018).
- [131] A. Milsted and G. Vidal, Tensor networks as conformal transformations, [arXiv:1805.12524](https://arxiv.org/abs/1805.12524).

- [132] A. Milsted and G. Vidal, Tensor networks as path integral geometry, [arXiv:1807.02501](#).
- [133] Y. Zou, A. Milsted, and G. Vidal, Conformal Fields and Operator Product Expansion in Critical Quantum Spin Chains, *Phys. Rev. Lett.* **124**, 040604 (2020).
- [134] A. Milsted and G. Vidal, Geometric interpretation of the multi-scale entanglement renormalization ansatz, [arXiv:1812.00529](#).
- [135] Q. Hu and G. Vidal, Spacetime Symmetries and Conformal Data in the Continuous Multiscale Entanglement Renormalization Ansatz, *Phys. Rev. Lett.* **119**, 010603 (2017).
- [136] A. R. Brown, M. H. Freedman, H. W. Lin, and L. Susskind, Effective geometry, complexity, and universality, [arXiv:2111.12700](#).
- [137] A. R. Brown, Polynomial equivalence of complexity geometries, [arXiv:2205.04485](#).